Pleiotropy analysis. We downloaded phenotype-associated SNPs and phenotype information from the National Human Genome Research Institute (NHGRI) GWAS catalogue database[26] on 31 January, 2013. We selected 4,676 significantly associated SNPs ($P < 5.0 \times 10^{-8}$) corresponding to 311 phenotypes (other than RA). We manually curated the phenotypes by combining the same but differently named phenotypes into a single phenotype (for example, from 'urate levels', 'uric acid levels' and 'renal function-related traits (urea)' to 'urate levels'), or splitting merged phenotypes into sub-categorical phenotypes (for example, from 'white blood cell types' into 'neutrophil counts', 'lymphocyte counts', 'monocyte counts', 'eosinophil counts' or 'basophil counts'). Lists of curated phenotypes and SNPs are available at http://plaza.umin.ac.jp/~yokada/datasource/software.htm.

For each of the selected NHGRI GWAS catalogue SNPs and the RA risk SNPs identified by our study (located outside of the MHC region), we defined the genetic region based on ±25 kb of the SNP or the neighbouring SNP positions in moderate linkage disequilibrium with it in Europeans or Asians ($r^2 > 0.50$). If multiple different SNPs with overlapping regions were registered for the same phenotype, they were merged into a single region. We defined 'region-based pleiotropy' as two phenotype-associated SNPs sharing part of their genetic regions or sharing any UCSC hg19 reference gene(s) that partly overlapped each of the regions (Extended Data Fig. 4a). We defined 'allele-based pleiotropy' as two phenotype-associated SNPs that were in linkage disequilibrium in Europeans or Asians ($r^2 > 0.80$). We defined the direction of an effect as 'concordant' with RA risk if the RA risk allele also leads to increased risk of the disease or increased dosage of the quantitative trait; similarly, we defined relationships as 'discordant' if the RA risk allele is associated with decreased risk of the disease phenotype (or if the RA risk allele leads to decreased dosage of the quantitative trait).

We evaluated statistical significance of region-based pleiotropy of the registered phenotypes with RA by a permutation procedure with $\times 10^7$ iterations. When one phenotype had n loci of which m loci were in region-based pleiotropy with RA, we obtained a null distribution of m by randomly selecting n SNPs from obtained NHGRI GWAS catalogue data and calculating the number of the observed region-based pleiotropy with RA for each of the iteration steps. For estimation of the null distribution, we did not include the SNPs associated with several autoimmune diseases that were previously reported to share pleiotropic associations with RA (Crohn's disease, type 1 diabetes, multiple sclerosis, coeliac disease, systemic lupus erythematosus, ulcerative colitis and psoriasis)[2].

Prioritization of biological candidate genes from RA risk loci. For RA risk SNPs outside of the MHC region, functional annotations were conducted by Annovar (hg19). RA risk SNPs were classified if any of the SNPs in linkage disequilibrium ($r^2 > 0.80$) in Europeans or Asians were annotated in order of priority of missense (or nonsense), synonymous or non-coding (with or without *cis*-eQTL) SNPs. We also applied this SNP annotation scheme to 10,000 randomly selected genome-wide common SNPs (MAF > 0.05 in Europeans or Asians).

We then assessed *cis*-eQTL effects by referring two eQTL data sets: the study for peripheral blood mononuclear cells (PBMCs) obtained from 5,311 European subjects[6] and newly generated cell-specific eQTL analysis for $CD4^+$ T cells and $CD14^+CD16^-$ monocytes from 212 European subjects (ImmVar project; T.R. *et al.*, manuscript submitted). When the RA risk SNP was not available in eQTL data sets, we alternatively used the results of best proxy SNPs in linkage disequilibrium with the highest r^2 value (>0.80). We applied the significance thresholds defined in the original studies (FDR $q < 0.05$ for PBMC eQTL and gene-based permutation $P < 0.05$ for cell-specific eQTL).

We obtained PID genes and their classification categories as defined by the International Union of Immunological Societies Expert Committee[14], downloaded cancer somatic mutation genes from the Catalogue of Somatic Mutations in Cancer (COSMIC) database[15], and downloaded knockout mouse phenotype labels and gene information from the Mouse Genome Informatics (MGI) database[16] on 31 January, 2013 (Supplementary Tables 2–5). We defined 377 RA risk genes included in the 100 RA risk loci (outside of the MHC region) according to the criteria described in the previous section (±25 kb or $r^2 > 0.50$), and evaluated overlap with PID categories, cancer phenotypes with registered somatic mutations, and phenotype labels of knockout mouse genes with human orthologues. Statistical significance of enrichment in gene overlap was assessed by a permutation procedure with $\times 10^6$ iterations. For each iteration step, we randomly selected 100 genetic loci matched for number of nearby genes with those in non-MHC 100 RA risk loci. When one gene category had m genes overlapping with RA risk genes, we obtained a null distribution of m by calculating the number of genes in the selected loci overlapping with RA risk genes for each iteration step.

We conducted molecular pathway enrichment analysis using MAGENTA software[9] and adopting Ingenuity and BIOCARTA databases as pathway information resources. We conducted two patterns of analyses by inputting genome-wide SNP P values of the current trans-ethnic meta-analysis (stage 1) and the previous meta-analysis of RA[2] separately. As the previous meta-analysis was conducted using imputed data based on HapMap Phase II panels, we re-performed the meta-analysis using the same subjects but with newly imputed genotype data based on the 1000 Genomes Project reference panel[11] to make SNP coverage conditions identical between the meta-analyses. Significance of the molecular pathway was evaluated by FDR q values obtained from $\times 10^5$ iterations of permutations.

We scored each of the genes included in the RA risk loci (outside of the MHC region) by adopting the following eight selection criteria and calculating the number of the satisfied criteria: (1) genes for which RA risk SNPs or any of the SNPs in linkage disequilibrium ($r^2 > 0.80$) with them were annotated as missense variants; (2) genes for which significant *cis*-eQTL of any of PBMCs, T cells or monocytes were observed for RA risk SNPs (FDR $q < 0.05$ for PBMCs and permutation $P < 0.05$ for T cells and monocytes); (3) genes prioritized by PubMed text mining using GRAIL[7] with gene-based $P < 0.05$; (4) genes prioritized by PPI network using DAPPLE[8] with gene-based $P < 0.05$; (5) PID genes[14]; (6) haematological cancer somatic mutation genes[15]; (7) genes for which ≥2 of associated phenotype labels ('haematopoietic system phenotype', 'immune system phenotype' and 'cellular phenotype'; $P < 1.0 \times 10^{-4}$) were observed for knockout mouse[16]; and (8) genes prioritized by molecular pathway analysis using MAGENTA[9], which were included in the significantly enriched pathways (FDR $q < 0.05$) with gene-based $P < 0.05$. Because these criteria showed weak correlations with each other ($R^2 < 0.26$; Extended Data Fig. 6c), each gene was given a score based on the number of criteria that were met (scores ranging from 0–8 for each gene). We defined the genes with a score ≥2 as 'biological RA risk genes'.

For each gene in RA risk loci, we evaluated whether the gene was the nearest gene to the RA risk SNP within the risk locus, or whether the RA risk SNP (or SNPs in linkage disequilibrium with it) of the gene overlapped with H3K4me3 histone peaks of cell types. The difference in proportions of genes that were the nearest gene to biological RA risk genes (score ≥2) and non-biological genes (score <2) was evaluated by using Fisher's exact test implemented in R statistical software (v.2.15.2). The difference in the proportions of genes overlapping with T_{reg} primary cell H3K4me3 peaks between biological and non-biological genes was assessed by a permutation procedure by shuffling the overlapping status of RA risk SNPs/loci with $\times 10^5$ iterations.

Drug target gene enrichment analysis. We obtained drug target genes and corresponding drug information from DrugBank[17] and the Therapeutic Targets Database (TTD)[18] on 31 January, 2013, as well as additional literature searches. We selected drug target genes that had pharmacological activities (for the genes from DrugBank) and human orthologues, and that were annotated to any of the approved, clinical trial or experimental drugs (Supplementary Table 6). We manually extracted drug target genes annotated to approved RA drugs on the basis of discussions with professional rheumatologists (Extended Data Fig. 7a). We extracted genes in direct PPI with biological RA risk genes by using the InWeb database[27]. To take account of potential dependence between PPI genes and drug target genes, overlap of biological RA risk genes and genes in direct PPI with them with drug target genes was assessed by a permutation procedure with $\times 10^5$ iterations.

Let x be the set of the biological RA risk genes and genes in direct PPI with them (n_x genes), y be the set of genes with protein products that are the direct target of approved RA drugs (n_y genes), and z be the set of genes with protein products that are the direct target of all approved drugs (n_z genes). We defined $n_{x\cap y}$ and $n_{x\cap z}$ as the numbers of genes overlapping between x and y and between x and z, respectively. For each of 10,000 iteration steps, we randomly selected a gene set of x' including n_x genes from the entire PPI network (12,735 genes). We defined $n_{x\cap y}'$ and $n_{x\cap z}'$ as the numbers of genes overlapping between x' and y, and between x' and z, respectively. The distributions of $n_{x\cap y}'$, $n_{x\cap z}'$ and $n_{x\cap y}'/n_{x\cap z}'$ obtained from the total iterations were defined as the null distributions of $n_{x\cap y}$, $n_{x\cap z}$, and $n_{x\cap y}/n_{x\cap z}$, respectively. Fold enrichment of overlap with approved RA drug target genes was defined as $n_{x\cap y}/m(n_{x\cap y}')$, where $m(t)$ represents the mean value of the distribution of t. Fold enrichment of overlap with approved all drug target genes was defined as $n_{x\cap z}/m(n_{x\cap z}')$. Relative fold enrichment of overlap with RA drug target genes and with all drug target genes was defined as $(n_{x\cap y}/n_{x\cap z})/m(n_{x\cap y}'/n_{x\cap z}')$. Significance of the enrichment was evaluated by one-sided permutation tests examining $n_{x\cap y}$, $n_{x\cap z}$, and $n_{x\cap y}/n_{x\cap z}$ in their null distributions.

Web resources. The following websites provide valuable additional resources. Summary statistics from the GWAS meta-analysis, source codes, and data sources have been deposited at http://plaza.umin.ac.jp/~yokada/datasource/software.htm; GARNET consortium, http://www.twmu.ac.jp/IOR/garnet/home.html; i2b2, https://www.i2b2.org/index.html; SLEGEN, http://www.lupusresearch.org/lupus-research/slegen.html; 1000 Genomes Project, http://www.1000genomes.org/; minimac, http://genome.sph.umich.edu/wiki/Minimac; mach2dat, http://www.sph.umich.edu/csg/abecasis/MACH/index.html; Annovar, http://www.openbioinformatics.org/annovar/; ImmVar, http://www.immvar.org/; NIH Roadmap Epigenomics Mapping Consortium, http://www.roadmapepigenomics.org/; NHGRI GWAS catalogue, http://www.genome.gov/GWAStudies/; COSMIC, http://cancer.sanger.ac.uk/cancergenome/projects/

cosmic/; MGI, http://www.informatics.jax.org/; MAGENTA, http://www.broadinstitute.org/mpg/magenta/; Ingenuity, http://www.ingenuity.com/; BIOCARTA, http://www.biocarta.com/; GRAIL, http://www.broadinstitute.org/mpg/grail/; DAPPLE, http://www.broadinstitute.org/mpg/dapple/dapple.php; R statistical software, http://www.r-project.org/; DrugBank, http://www.drugbank.ca/; TTD, http://bidd.nus.edu.sg/group/ttd/ttd.asp.

24. Arnett, F. C. *et al.* The American Rheumatism Association 1987 revised criteria for the classification of rheumatoid arthritis. *Arthritis Rheum.* **31,** 315–324 (1988).
25. Okada, Y. *et al.* Meta-analysis identifies multiple loci associated with kidney function-related traits in east Asian populations. *Nature Genet.* **44,** 904–909 (2012).
26. Hindorff, L. A. *et al.* Potential etiologic and functional implications of genome-wide association loci for human diseases and traits. *Proc. Natl Acad. Sci. USA* **106,** 9362–9367 (2009).
27. Lage, K. *et al.* A human phenome-interactome network of protein complexes implicated in genetic disorders. *Nature Biotechnol.* **25,** 309–316 (2007).
28. Ueda, H. *et al.* Association of the T-cell regulatory gene CTLA4 with susceptibility to autoimmune disease. *Nature* **423,** 506–511 (2003).
29. Elliott, P. *et al.* Genetic loci associated with C-reactive protein levels and risk of coronary heart disease. *J. Am. Med. Assoc.* **302,** 37–48 (2009).
30. Cortes, A. *et al.* Identification of multiple risk variants for ankylosing spondylitis through high-density genotyping of immune-related loci. *Nature Genet.* **45,** 730–738 (2013).

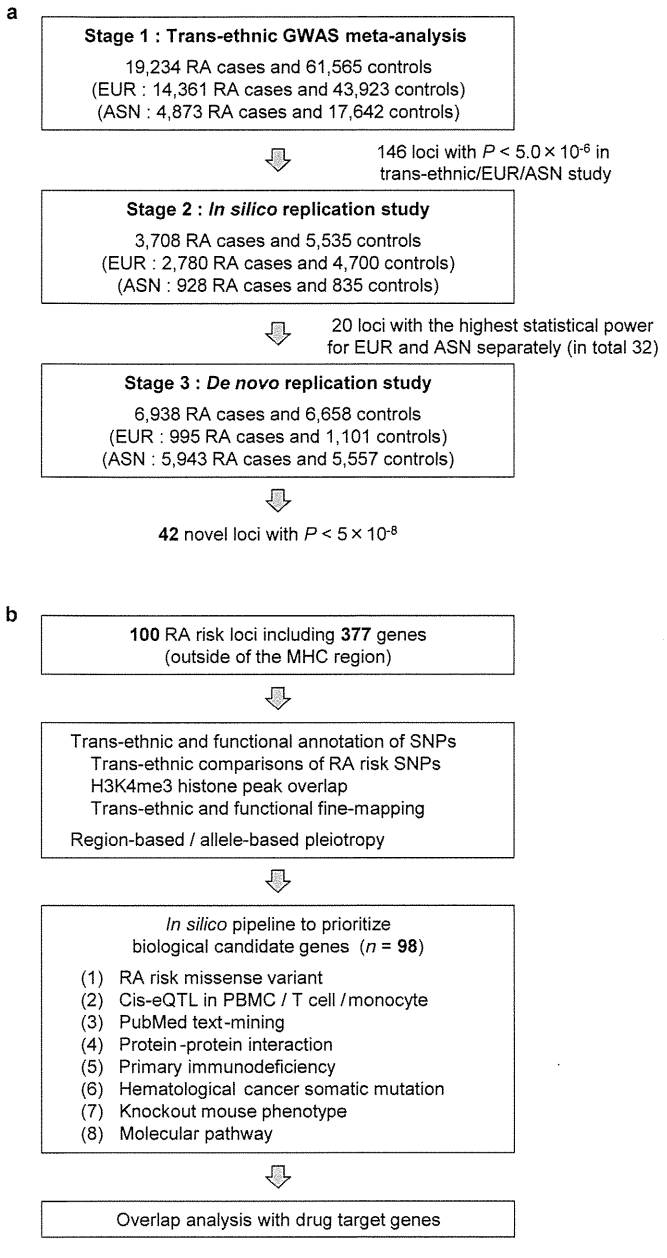

Extended Data Figure 1 | An overview of the study design. **a**, We conducted a three-stage trans-ethnic meta-analysis in total of 29,880 RA cases and 73,758 controls of European (EUR) and Asian (ASN) ancestry. The stage 1 GWAS meta-analysis included 19,234 RA cases and 61,565 controls from 22 studies, which was followed by the stage 2 *in silico* replication study (3,708 RA cases and 5,535 controls) and stage 3 *de novo* replication study (6,938 RA cases and 6,658 controls). In the combined study of stages 1–3, we identified 42 novel RA risk loci, which increased the total number of RA risk loci to 101. **b**, Using the 100 RA risk loci (outside of the MHC region), we conducted trans-ethnic and functional annotation of the RA risk SNPs. We constructed an *in silico* bioinformatics pipeline to prioritize biological candidate genes. We adopted eight criteria to score each of 377 genes in the RA risk loci: (1) RA risk missense variant; (2) *cis*-eQTL; (3) PubMed text mining; (4) PPI; (5) PID; (6) haematological cancer somatic mutation; (7) knockout mouse phenotype; and (8) molecular pathway. Our study also demonstrated that these biological candidate genes in RA risk loci are significantly enriched in overlap with target genes for approved RA drugs.

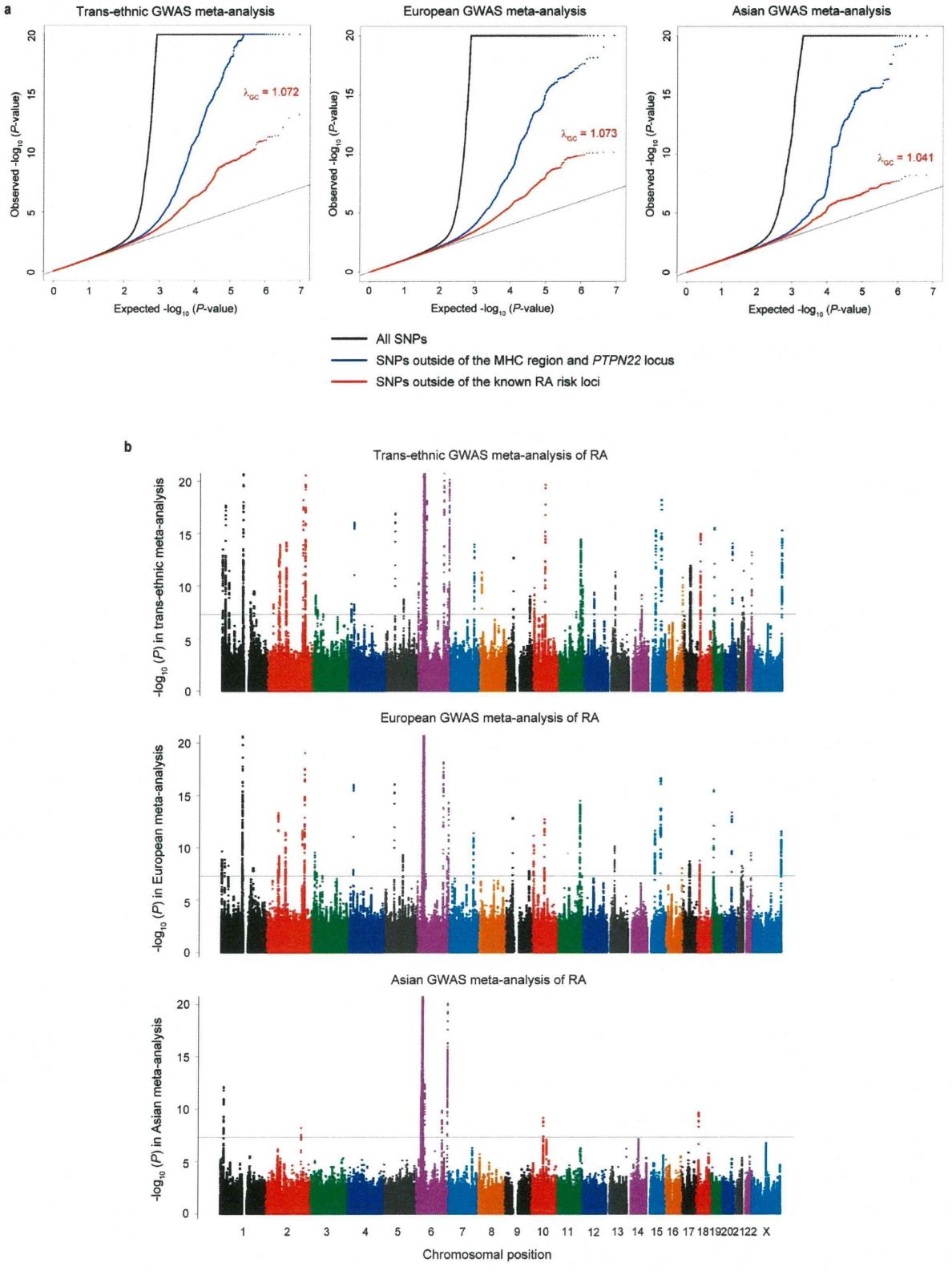

Extended Data Figure 2 | Quantile–quantile plots and Manhattan plots of *P* values in the GWAS meta-analysis. **a**, Quantile–quantile plots of *P* values in the stage 1 GWAS meta-analysis for trans-ethnic, European and Asian ancestries. The *x*-axis indicates the expected $-\log_{10}$ (*P* values). The *y*-axis indicates the observed $-\log_{10}$ (*P* values) after the application of double GC correction. The SNPs for which observed *P* values were less than 1.0×10^{-20} are indicated at the upper limit of each plot. Black, blue and red dots represent the association results of all SNPs, SNPs outside of the MHC region and *PTPN22* locus, and SNPs outside of the known RA risk loci, respectively. Double GC correction was applied based on the inflation factor, λ_{GC}, which was estimated from the SNPs outside of the known RA loci and indicated in each plot. **b**, Manhattan plots of *P* values in the stage 1 GWAS meta-analysis for trans-ethnic, European and Asian ancestries. The *y*-axis indicates the $-\log_{10}$ (*P* values) of genome-wide SNPs in each GWAS meta-analysis. The horizontal grey line represents the genome-wide significance threshold of $P = 5.0 \times 10^{-8}$. The SNPs for which *P* values were less than 1.0×10^{-20} are indicated at the upper limit of each plot.

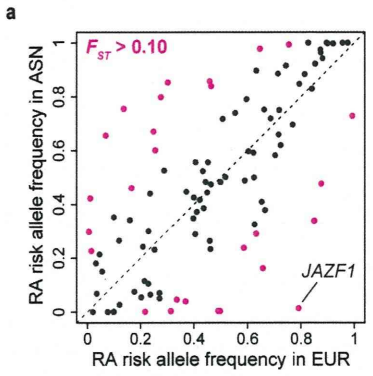

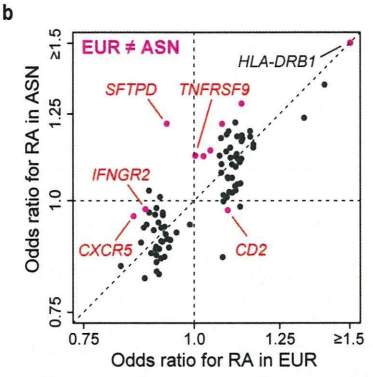

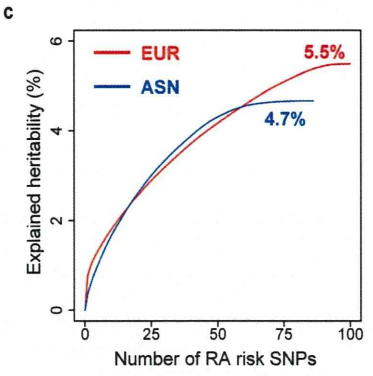

d

Cell types	*P* for H3K4me3 enrichment
T_{reg} primary cells	$\leq 1.0\times10^{-5}$
$CD4^+$ memory primary cells	3.0×10^{-5}
$CD4^+$ naive primary cells	0.0041
$CD8^+$ memory primary cells	0.0065
Smooth muscle, rectal	0.034
Mucosa, colon	0.038
$CD8^+$ naive primary cells	0.12
Mucosa, stomach	0.13
$CD34^+$ primary cells	0.18
$CD34^+$ cultured cells	0.19
Mobilized $CD34^+$ primary cells	0.19
$CD19^+$ primary cells	0.24
$CD3^+$ primary cells	0.30
Mucosa, duodenum	0.40
Muscle satellite cultured cells	0.46
Cingulate gyrus (brain)	0.53
Skeletal muscle	0.77
Mucosa, rectal	0.77
Smooth muscle, colon	0.79
Mesenchymal stem cells (adipose)	0.81
Adipose nuclei	0.84
Smooth muscle, duodenum	0.85
Mid frontal lobe (brain)	0.86
Hippocampus middle (brain)	0.91
Mesenchymal stem cells (bone marrow)	0.91
Pancreatic islets	0.93
Inferior temporal lobe (brain)	0.93
Substantia nigra (brain)	0.93
Adult kidney	0.94
Adult liver	0.95
Mesenchymal stem cells (adipocyte)	0.98
Mesenchymal stem cells (chondrocytes)	0.99
Anterior caudate (brain)	0.99
Smooth muscle, stomach	0.99

e

31 RA risk loci with $P < 10^{-3}$ in EUR and ASN meta-analysis

21.9 SNPs/locus in LD (r^2>0.8) in EUR

37.3 SNPs/locus in LD (r^2>0.8) in ASN

15.0 SNPs/locus in LD (r^2>0.8) in EUR and ASN

10 RA risk loci significantly enriched with T_{reg} primary cell H3K4me3 peaks ($P < 0.05$)

10.4 SNPs/locus in LD (r^2>0.8) in EUR and ASN

5.9 SNPs/locus in LD (r^2>0.8) in EUR and ASN and overlapping with H3K4me3 peaks

f

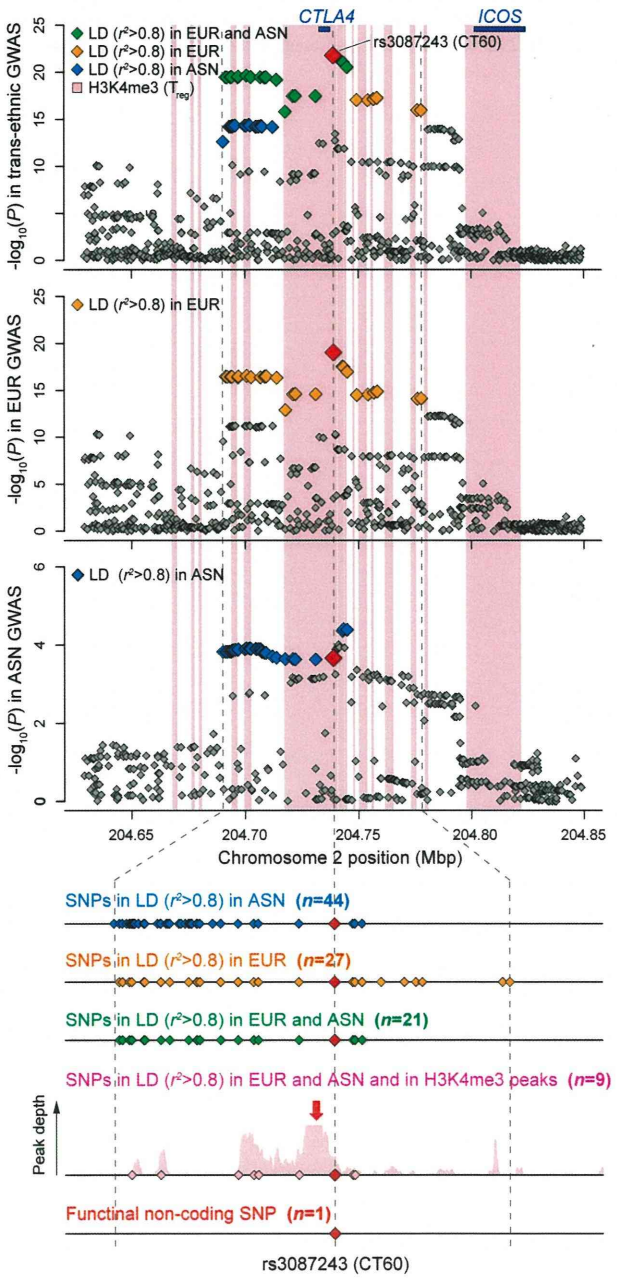

Extended Data Figure 3 | Trans-ethnic and functional annotation of RA risk SNPs. **a**, **b**, Comparisons of RAF and OR values between individuals of European (EUR) and Asian (ASN) ancestry from the stage 1 GWAS meta-analysis. ORs were defined based on minor alleles in Europeans. SNPs with $F_{ST} > 0.10$ or SNPs in which the 95% CI of the OR did not overlap between Europeans and Asians are coloured. OR of the SNP in the *HLA-DRB1* locus ($\geq$1.5) is plotted at the upper limits of the *x*- and *y*-axes. Five loci demonstrated population-specific associations ($P < 5.0 \times 10^{-8}$ in one population but $P > 0.05$ in the other population without overlap of the 95% CI of the OR) are highlighted by red labels (rs227163 at *TNFRSF9*, rs624988 at *CD2*, rs726288 at *SFTPD*, rs10790268 at *CXCR5* and rs73194058 at *IFNGR2*). **c**, Cumulative curve of explained heritability in each population. **d**, Enrichment analysis for overlap of RA risk SNPs with H3K4me3 peaks in cell types. The most significant cell type is T_{reg} primary cells. **e**, Number of SNPs in the process of trans-ethnic and functional fine mapping. For 31 loci in which the risk SNPs yielded $P < 1.0 \times 10^{-3}$ in both populations (stage 1 GWAS), the number of candidate causal variants was reduced by 40–70% when confined by SNPs in linkage disequilibrium with the RA risk SNPs ($r^2 > 0.80$) in both populations (on average, from 21.9 or 37.3 SNPs in linkage disequiliberium in Europeans or Asians, to 15.0 SNPs in linkage disequilibrium in both populations). Further, for 10 loci in which candidate causal variants significantly overlapped with H3K4me3 peaks in T_{reg} cells ($P < 0.05$), the average number of SNPs was further reduced by half again, from 10.4 to 5.9. **f**, Fine mapping in the *CTLA4* locus, where the functional non-coding variant of CT60 (rs3087243)[28] showed the most significant association with RA. The top three panels indicate regional SNP associations of the locus in the stage 1 GWAS meta-analysis for trans-ethnic, European and Asian ancestries, respectively. The bottom panel indicates the change in the number of the candidate causal variants in each process of fine mapping. Trans-ethnic fine mapping of candidate causal variants decreased the number of candidate variants from 44 (linkage disequilibrium in Asians) and 27 (linkage disequilibrium in Europeans) to 21 (linkage disequilibrium in both populations). As these SNPs were significantly enriched in overlap with H3K4me3 peaks in T_{reg} cells compared with the surrounding SNPs ($P = 0.037$), we confined the candidate variants into nine by additionally selecting the SNPs included in H3K4me3 peaks. CT60 was included in these finally selected nine SNPs, and also located at the vicinity of a H3K4me3 peak summit (indicated by a red arrow).

a

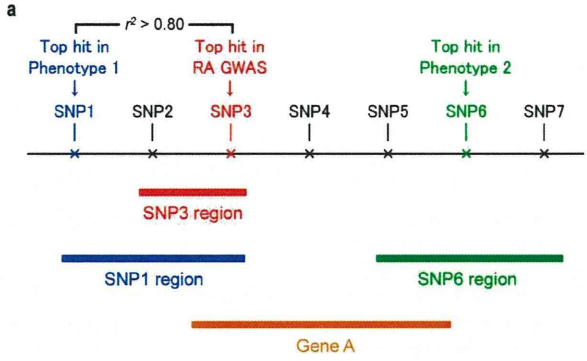

RA and Phenotype 1 : Both region-based and allele-based pleiotropy.

RA and Phenotype 2 : Region-based pleiotropy only.

b

Phenotype in GWAS catalogue	No. loci	Region-based pleiotropy		Allele-based pleiotropy
		No. overlap	P-value	
Type 1 diabetes	42	15	$<1.0\times10^{-7}$	7
Crohn's disease	79	15	$<1.0\times10^{-7}$	4
Systemic lupus erythematosus	22	10	$<1.0\times10^{-7}$	6
Celiac disease	26	10	$<1.0\times10^{-7}$	3
Vitiligo	23	9	$<1.0\times10^{-7}$	3
Primary biliary cirrhosis	22	7	2.4×10^{-6}	3
Alopecia areata	5	4	4.5×10^{-6}	0
Ulcerative colitis	52	9	2.5×10^{-5}	3
Multiple sclerosis	52	9	2.5×10^{-5}	2
Chronic lymphocytic leukemia	9	4	9.1×10^{-5}	0
Kawasaki disease	5	3	2.4×10^{-4}	2
Graves' disease	5	3	2.4×10^{-4}	1
Systemic sclerosis	5	3	2.4×10^{-4}	1
Fibrinogen	8	3	0.0012	1
Asthma	17	4	0.0015	2
Psoriasis	18	4	0.0019	1
Hypothyroidism	4	2	0.0041	2
Basal cell carcinoma	5	2	0.0069	0
Neutrophil count	5	2	0.0069	0
HDL cholesterol	46	5	0.014	1
Eosinophil counts	8	2	0.018	1
C-reactive protein	20	3	0.020	1
Melanoma	11	2	0.034	0
Myasthenia gravis	2	1	0.039	1
Primary sclerosing cholangitis	2	1	0.039	0
Soluble ICAM-1	2	1	0.039	0

c

SNP	Chr.	Position (bp)	A1/A2	Gene	Phenotype	Direction
chr1:2523811	1	2,523,811	G/A	*TNFRSF14-MMEL1*	Multiple sclerosis	Concordant
rs2476601	1	114,377,568	A/G	*PTPN22*	Hypothyroidism	Concordant
					Myasthenia gravis	Concordant
					Crohn's disease	Discordant
					Type 1 diabetes	Concordant
rs2228145	1	154,426,970	A/C	*IL6R*	C-reactive protein	Concordant
					Asthma	Discordant
					sIL-6R	Discordant
					Fibrinogen	Concordant
rs2317230	1	157,674,997	T/G	*FCRL3*	Graves' disease	Concordant
rs34695944	2	61,124,850	C/T	*REL*	Hodgkin lymphoma	Concordant
					Psoriasis	Discordant
rs11889341	2	191,943,742	T/C	*STAT4*	Systemic sclerosis	Concordant
					Systemic lupus erythematosus	Concordant
rs3087243	2	204,738,919	G/A	*CTLA4*	Type 1 diabetes	Concordant
rs11933540	4	26,120,001	C/T	*C4orf52*	Type 1 diabetes	Concordant
rs17264332	6	138,005,515	G/A	*TNFAIP3*	Celiac disease	Concordant
					Ulcerative colitis	Concordant
rs7752903	6	138,227,364	G/T	*TNFAIP3*	Systemic lupus erythematosus	Concordant
chr7:128580042	7	128,580,042	G/A	*IRF5*	Ulcerative colitis	Concordant
					Systemic lupus erythematosus	Concordant
rs2736337	8	11,341,880	C/T	*BLK*	Kawasaki disease	Concordant
					Systemic lupus erythematosus	Concordant
rs1516971	8	129,542,100	T/C	*PVT1*	Ovarian cancer	Concordant
					Crohn's disease	Concordant
rs947474	10	6,390,450	A/G	*PRKCQ*	Type 1 diabetes	Concordant
rs2671692	10	50,097,819	A/G	*WDFY4*	Systemic lupus erythematosus	Concordant
rs726288	10	81,706,973	T/C	*SFTPD*	Serum SP-D levels	Concordant
rs4409785	11	95,311,422	C/T	*CEP57*	Vitiligo	Concordant
rs10790268	11	118,729,391	G/A	*CXCR5*	Primary biliary cirrhosis	Concordant
rs61432431	11	128,322,622	C/T	*ETS1*	Systemic lupus erythematosus	Concordant
rs773125	12	56,394,954	A/G	*CDK2*	Polycystic ovary syndrome	Discordant
					Vitiligo	Discordant
					Type 1 diabetes	Discordant
rs10774624	12	111,833,788	G/A	*SH2B3-PTPN11*	Eosinophil counts	Concordant
					Hypothyroidism	Concordant
					Platelet-related traits	Concordant
					Type 1 diabetes	Concordant
					Blood pressure and hypertension	Concordant
					Vitiligo	Concordant
					Retinal vascular caliber	Concordant
					CKD	Concordant
					Celiac disease	Concordant
rs1950897	14	68,760,141	T/C	*RAD51B*	Primary biliary cirrhosis	Concordant
rs13330176	16	86,019,087	A/T	*IRF8*	Multiple sclerosis	Concordant
chr17:38031857	17	38,031,857	G/T	*IKZF3-CSF3*	Primary biliary cirrhosis	Concordant
					Ulcerative colitis	Concordant
					Crohn's disease	Concordant
					Asthma	Discordant
					Type 1 diabetes	Concordant
rs4239702	20	44,749,251	C/T	*CD40*	Kawasaki disease	Concordant
rs2236668	21	45,650,009	C/T	*ICOSLG-AIRE*	Celiac disease	Concordant
rs11089637	22	21,979,096	C/T	*UBE2L3-YDJC*	Crohn's disease	Concordant
					HDL	Discordant

d

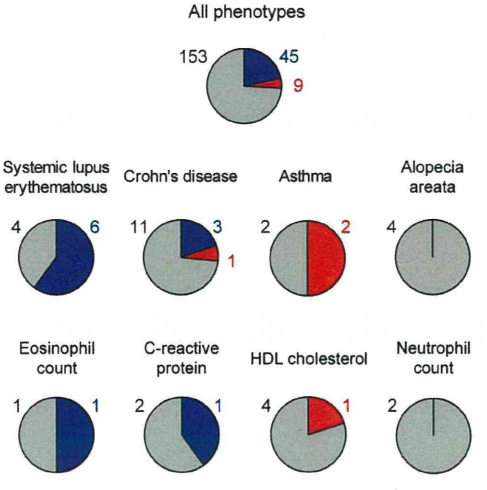

Region- and Allele-based pleiotropy (concordant direction)

Region- and Allele-based pleiotropy (discordant direction)

Region-based pleiotropy only

e

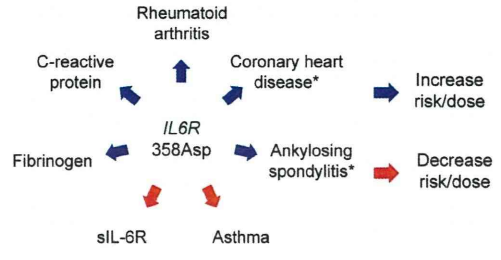

Extended Data Figure 4 | Pleiotropy of RA risk SNPs. **a**, Definition of region-based and allele-based pleiotropy. For each of the RA risk SNPs and SNPs registered in the NHGRI GWAS catalogue (outside of the MHC region), we defined the region on the basis of ±25 kb of the SNP or the neighbouring SNP positions in moderate linkage disequilibrium with it in Europeans or Asians ($r^2 > 0.50$). We defined 'region-based pleiotropy' as two phenotype-associated SNPs sharing part of their genetic regions or any UCSC hg19 reference gene(s) partly overlapping with each of the regions. We defined 'allele-based pleiotropy' as two phenotype-associated SNPs in linkage disequilibrium in Europeans or Asians ($r^2 > 0.80$). **b**, Region-based pleiotropy of the RA risk loci. We found two-thirds of RA risk loci ($n = 66$) demonstrated region-based pleiotropy with other human phenotypes. Phenotypes which showed region-based pleiotropy with RA risk loci are indicated ($P < 0.05$). **c**, Allele-based pleiotropy of the RA risk loci. Allele-based pleiotropy with discordant directional effects to RA risk SNPs are indicated in grey. **d**, Relative proportions of pleiotropic effects (that is, regions and alleles that influence multiple phenotypes) between RA risk loci and 311 phenotypes from the NHGRI GWAS catalogue. Representative examples of disease and biomarker phenotypes are shown. One-quarter of the observed region-based pleiotropic associations (26% = 54/207) were also annotated as having allele-based pleiotropy, although their proportions and directional effects varied among phenotypes. **e**, Allele-based pleiotropy of *IL6R* 358Asp (rs2228145 (A))[5] on multiple disease phenotypes, including increased risk of RA, ankylosing spondylitis and coronary heart disease (asterisks indicate associations obtained from the literature[29,30]) and protection from asthma, as well as levels of biomarkers (increased C-reactive protein (CRP) and fibrinogen but decreased soluble interleukin-6 receptor (sIL6R)).

a

RA risk SNP	r^2	Gene	Missense variants
rs2301888	0.95	*PADI4*	Gly55Ser, Val82Ala, Gly112Ala
rs2476601	1.00	*PTPN22*	Arg620Trp
rs2228145	1.00	*IL6R*	Asp358Ala
rs9826828	0.92	*NCK1*	Ala116Val
	1.00	*NFKBIE*	Val194Ala, Pro175Leu
rs2233424	0.94	*TCTE1*	Arg59His
	0.88	*AARS2*	Val730Met
rs7752903	1.00	*TNFAIP3*	Phe127Cys
rs2671692	0.84	*WDFY4*	Arg1816Gln
rs6479800	0.88	*RTKN2*	Ala288Thr
rs508970	0.90	*CD5*	Ala471Val
rs10774624	0.86	*SH2B3*	Trp262Arg
rs3783782	1.00	*PRKCH*	Val374Ile
rs2582532	1.00	*AHNAK2*	Gly1901Ser
chr17:38031857	0.99	*ZPBP2*	Ser151Ile
	0.99	*GSDMB*	Pro298Ser, Gly291Arg
rs34536443	0.87	*TYK2*	Pro1104Ala
rs2236668	0.94	*ICOSLG*	Trp353Arg
rs5987194	0.96	*IRAK1*	Phe196Ser, Ser453Leu

b

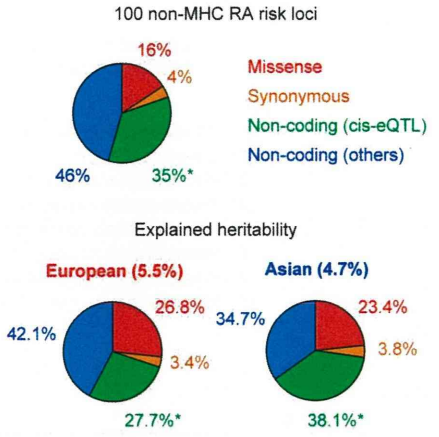

c

	PID classification	No. PID genes	No. overlap with RA genes	Overlap genes	P-value
	All PID genes	194	14	-	1.2×10^{-4}
I	Combined immunodeficiencies	43	3	*PTPRC, RAG1/2, CD40*	0.046
II	Well-defined syndromes	25	2	*ATM, TYK2*	0.12
III	Primary antibody deficiencies	21	2	*CD40, UNG*	0.030
IV	Immune dysregulation	21	4	*CASP8, CASP10, AIRE, IL2RA*	0.0033
V	Phagocyte defects	33	2	*IFNGR2, IRF8*	0.16
VI	Innate immunity	19	0	-	1.0
VII	Autoinflammatory	13	1	*MVK*	0.16
VIII	Complement deficiencies	27	1	*C5*	0.33

d

Cancer type	No. cancer somatic mutation genes	No. overlap with RA genes	Overlap genes	P-value
All cancers	444	23	-	4.7×10^{-5}
Hematological cancers	251	17	-	1.2×10^{-4}
Non-hematological cancers	221	6	-	0.56
Hodgkin lymphoma	10	2	*REL, TNFAIP3*	0.010
B cell non-Hodgkin lymphoma	8	2	*DDX6, FCRL4*	0.015
Non-Hodgkin lymphoma	21	2	*FGFR1OP, HSP90AB1*	0.067
Acute lymphocytic leukemia	29	3	*FCGR2B, AFF3, CDK6*	0.079
Acute myelogenous leukemia	68	2	*ACSL6, PTPN11*	0.47

e

Konckout mouse phenotype category	No. kockout mouse genes with human ortholog	No. overlap with RA genes	P-value
Hematopoietic system phenotype	**2,159**	**86**	**7.0×10^{-6}**
Immune system phenotype	**2,622**	**94**	**1.2×10^{-5}**
Cellular phenotype	**2,961**	**97**	**0.0015**
Liver/biliary system phenotype	982	35	0.0091
Renal/urinary system phenotype	1,028	35	0.011
Endocrine/exocrine gland phenotype	1,453	45	0.020
Respiratory system phenotype	1,097	31	0.028
Tumorigenesis	807	30	0.049
Normal phenotype	1,599	42	0.18
Homeostasis/metabolism phenotype	3,356	88	0.20
Integument phenotype	1,455	35	0.27
Pigmentation phenotype	355	9	0.31
Cardiovascular system phenotype	1,987	42	0.51
Skeleton phenotype	1,435	34	0.57
Other phenotype	258	6	0.57
No phenotypic analysis	1,053	21	0.59
Mortality/aging	3,952	93	0.75
Adipose tissue phenotype	617	12	0.78
Growth/size phenotype	3,061	67	0.79
Digestive/alimentary phenotype	1,128	22	0.80
Reproductive system phenotype	1,730	37	0.81
Limbs/digits/tail phenotype	748	13	0.82
Taste/olfaction phenotype	123	1	0.85
Hearing/vestibular/ear phenotype	557	8	0.88
Embryogenesis phenotype	1,535	30	0.92
Behavior/neurological phenotype	2,465	46	0.94
Nervous system phenotype	2,805	53	0.95
Craniofacial phenotype	951	15	0.96
Muscle phenotype	1,198	21	0.96
Vision/eye phenotype	1,214	21	0.99

f

Database	Molecular pathway	Pathway enrichment (FDR q) Current study	Previous study
BIOCARTA	B Lymphocyte Cell Surface Molecules	**2.0×10^{-4}**	0.26
BIOCARTA	T Cytotoxic Cell Surface Molecules	**3.3×10^{-4}**	**0.032**
BIOCARTA	T Helper Cell Surface Molecules	**4.0×10^{-4}**	**0.030**
BIOCARTA	Th1/Th2 Differentiation	**0.0025**	**0.0063**
Ingenuity	IL-10.Signaling	**0.0026**	0.46
Ingenuity	Interferon.Signaling	**0.0028**	0.13
Ingenuity	GM-CSF.Signaling	**0.0031**	0.43
Ingenuity	T.Cell.Receptor.Signaling	**0.0034**	**0.029**
BIOCARTA	NO2-dependent IL 12 Pathway in NK cells	**0.0044**	0.06
BIOCARTA	IL-22 Soluble Receptor Signaling	**0.0046**	0.39
BIOCARTA	The Co-Stimulatory Signal During T-cell Activation	**0.0046**	0.06
BIOCARTA	Selective expression of chemokine receptors during T-cell polarization	**0.0048**	0.21
Ingenuity	Hepatic.Fibrosis.Hepatic.Stellate.Cell.Activation	**0.0073**	**0.0060**
Ingenuity	p38.MAPK.Signaling	**0.0076**	0.19
Ingenuity	Neuregulin.Signaling	**0.0079**	0.51
Ingenuity	IL-6.Signaling	**0.0082**	0.11
Ingenuity	Glucocorticoid.Receptor.Signaling	**0.0090**	0.18
BIOCARTA	IL-6 signaling	**0.0091**	0.50
BIOCARTA	Influence of Ras and Rho proteins on G1 to S Transition	**0.016**	0.38
BIOCARTA	IL-3 signaling	**0.018**	0.64
BIOCARTA	Adhesion and Diapedesis of Granulocytes	**0.018**	0.15
BIOCARTA	RB Tumor Suppressor/Checkpoint Signaling in response to DNA damage	**0.018**	0.15
Ingenuity	Fc.Epsilon.RI.Signaling	**0.022**	0.19
Ingenuity	JAK.Stat.Signaling	**0.023**	0.48
Ingenuity	IL-2.Signaling	**0.026**	0.17
Ingenuity	PPAR.Signaling	**0.026**	0.24
BIOCARTA	IL-2 Receptor Beta Chain in T cell Activation	**0.027**	0.39
BIOCARTA	Cyclins and Cell Cycle Regulation	**0.028**	0.16
Ingenuity	Leukocyte.Extravasation.Signaling	**0.028**	0.45
BIOCARTA	p53 Signaling Pathway	**0.028**	0.40
BIOCARTA	Role of ERBB2 in Signal Transduction and Oncology	**0.028**	0.51
Ingenuity	B.Cell.Receptor.Signaling	**0.028**	0.45
BIOCARTA	CD40L Signaling	**0.029**	0.16
BIOCARTA	Cells and Molecules involved in local acute inflammatory response	**0.034**	0.40
BIOCARTA	Antigen Dependent B Cell Activation	**0.036**	0.06
BIOCARTA	Adhesion and Diapedesis of Lymphocytes	**0.043**	0.60
BIOCARTA	MAPKinase Signaling	**0.044**	0.76
BIOCARTA	Phosphorylation of MEK1 by cdk5/p35 down regulates the MAP kinase	**0.044**	0.59
Ingenuity	NFKB.Signaling	**0.045**	0.05
Ingenuity	Aryl.Hydrocarbon.Receptor.Signaling	**0.048**	0.33
Ingenuity	PDGF.Signaling	**0.049**	0.30

Extended Data Figure 5 | Overlap of RA risk SNPs with biological resources. **a**, Missense variants in linkage disequilibrium ($r^2 > 0.80$ in Europeans or Asians) with RA risk SNPs. When multiple missense variants are in linkage disequilibrium with the RA risk SNP, the highest r^2 value is indicated. **b**, Functional annotation of the SNPs in 100 non-MHC RA risk loci, including the relative proportion of heritability explained by SNP annotations. Although 44% of all RA risk SNPs had *cis*-eQTL, 9 of them overlapped with missense or synonymous variants but 35 of them did not overlap as indicated by asterisks. A list of *cis*-eQTL SNPs and genes can be found in Extended Data Table 2. **c**, Overlap of RA risk genes with human PID and defined categories. **d**, Overlap of RA risk genes with cancer somatic mutation genes. In addition to the categories of all cancers, haematological cancers and non-haematological cancers, cancer types that showed overlap with ≥2 of RA risk genes are indicated. **e**, Overlap of RA risk genes with knockout mouse phenotypes. Knockout mouse phenotypes that satisfied significant enrichment with RA risk genes are indicated in bold ($P < 0.05/30 = 0.0017$). **f**, Molecular pathway analysis of RA GWAS results. Molecular pathways that showed significant enrichment in either the current stage 1 trans-ethnic GWAS meta-analysis or the previous GWAS meta-analysis of RA[2] are indicated in bold (FDR $q < 0.05$).

a

Biological RA risk gene prioritization criteria

(1) RA risk missense variant (n = 19)
(2) Cis-eQTL (n = 51)
(3) PubMed text-mining (n = 90)
(4) Protein-protein interaction (n = 63)
(5) Primary immunodeficiency (n = 15)
(6) Hematological cancer (n = 17)
(7) Knockout mouse phenotype (n = 86)
(8) Molecular pathway (n = 35)

b

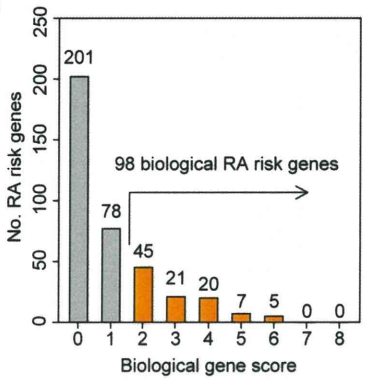

c

Correlation of prioritization criteria of biological genes from RA risk loci (R^2)	RA risk missense variant	Cis-eQTL	PubMed text-mining	Protein-protein interaction	Primary immunodeficiency	Hematological cancer	Knockout mouse phenotype	Molecuular pathway
RA risk missense variant	-	0.01	0.03	0.02	0.00	0.00	0.02	0.01
Cis-eQTL	0.01	-	0.05	0.01	0.01	0.00	0.02	0.01
PubMed text-mining	0.03	0.05	-	0.10	0.06	0.03	0.26	0.14
Protein-protein interaction	0.02	0.01	0.10	-	0.04	0.01	0.07	0.06
Primary immunodeficiency	0.00	0.01	0.06	0.04	-	0.00	0.08	0.07
Hematological cancer	0.00	0.00	0.03	0.01	0.00	-	0.03	0.04
Knockout mouse phenotype	0.02	0.02	0.26	0.07	0.08	0.03	-	0.21
Molecular pathway	0.01	0.01	0.14	0.06	0.07	0.04	0.21	-

d

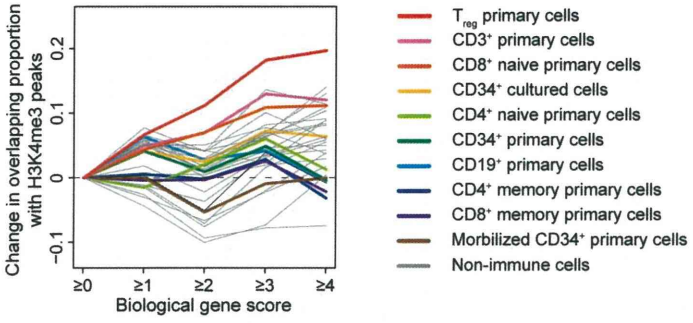

Extended Data Figure 6 | Prioritization of biological candidate genes from RA risk loci. **a**, Prioritization criteria of biological candidate genes from RA risk loci. **b**, Histogram distribution of gene scores. The 98 genes with score ≥2 (orange) were defined as 'biological RA risk genes'. **c**, Correlations of biological candidate gene prioritization criteria. **d**, Change in the overlapping proportions of genes with H3K4me3 peaks by cell type according to score increases. When RA risk SNP of the locus (or SNP in linkage disequilibrium) overlapped with H3K4me3 peaks, genes in the locus were defined as overlapping.

a

RA drug category	Generic name	Target gene
Biologics	Etanercept	
	Infliximab	
	Adalimumab	*TNF*
	Golimumab	
	Certolizumab pegol	
	Abatacept	*CD80, CD86*
	Anakinra	*IL1R1*
	Rituximab	*MS4A1*
	Tocilizumab	*IL6R*
DMARDs	Auranofin	*PRDX5, IKBKB*
	Azathioprine	*HPRT1*
	Cyclophosphamide	-
	Cyclosporine	*CAMLG, PPP3R2*
	Iguratimod (T-614)	*ELANE, PTGS2*
	Leflunomide	*DHODH*
	Methotrexate	*DHFR*
	Sulfasalazine	*ALOX5, PTGS1, PTGS2, PPARG*
	Tacrolimus	*FKBP1A*
	Temsirolimus	*MTOR*
	Tofacitinib (CP-690,550)	*JAK1, JAK2, JAK3*
Steroids	Prednisolone	*NR3C1*
	Methylprednisolone	*NR3C1*
	Desoxycorticosterone Pivalate	*NR3C2*
Others	Hydroxychloroquine	*TLR7, TLR9*

b

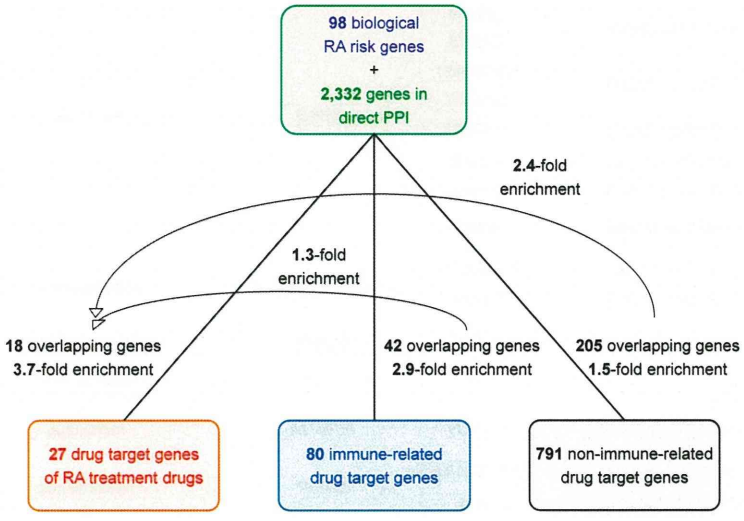

c

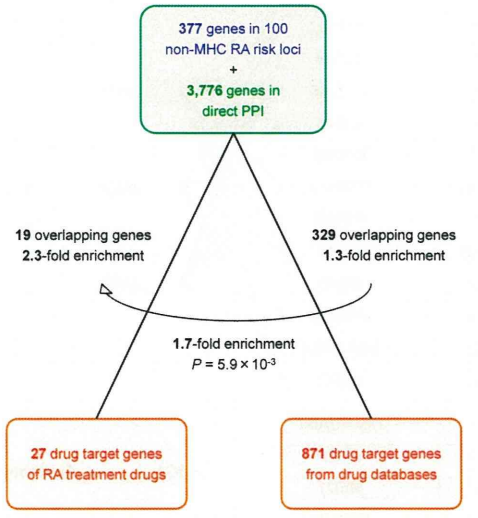

Extended Data Figure 7 | Overlap of all genes in the RA risk loci with drug target genes. **a**, Approved RA drugs and target genes. DMARDs, disease-modifying antirheumatic drugs. **b**, Overlap analysis stratified by immune-related and non-immune-related drug target genes. We made a list of 583 immune-related genes based on Gene Ontology (GO) pathways named 'immune-' or 'immuno-' and found that the majority of drug target genes (791/871 = 91%) were not immune-related. **c**, Overlap of all 377 genes included in 100 RA risk loci (outside of the MHC region) plus 3,776 genes in direct PPI with them and drug target genes. We found overlap of 19 genes from the 27 drug target genes of approved RA drugs (2.3-fold enrichment, $P < 1.0 \times 10^{-5}$). All 871 drug target genes (regardless of disease indication) overlap with 329 genes from the PPI network, which is 1.3-fold more enrichment than expected by chance alone ($P < 1.0 \times 10^{-5}$), but less than 1.7-fold enrichment compared with RA drugs ($P = 0.0059$). We note that this enrichment of drug–gene pairs was less apparent compared with that obtained from the expanded PPI network generated from 98 biological candidate genes (Fig. 3b).

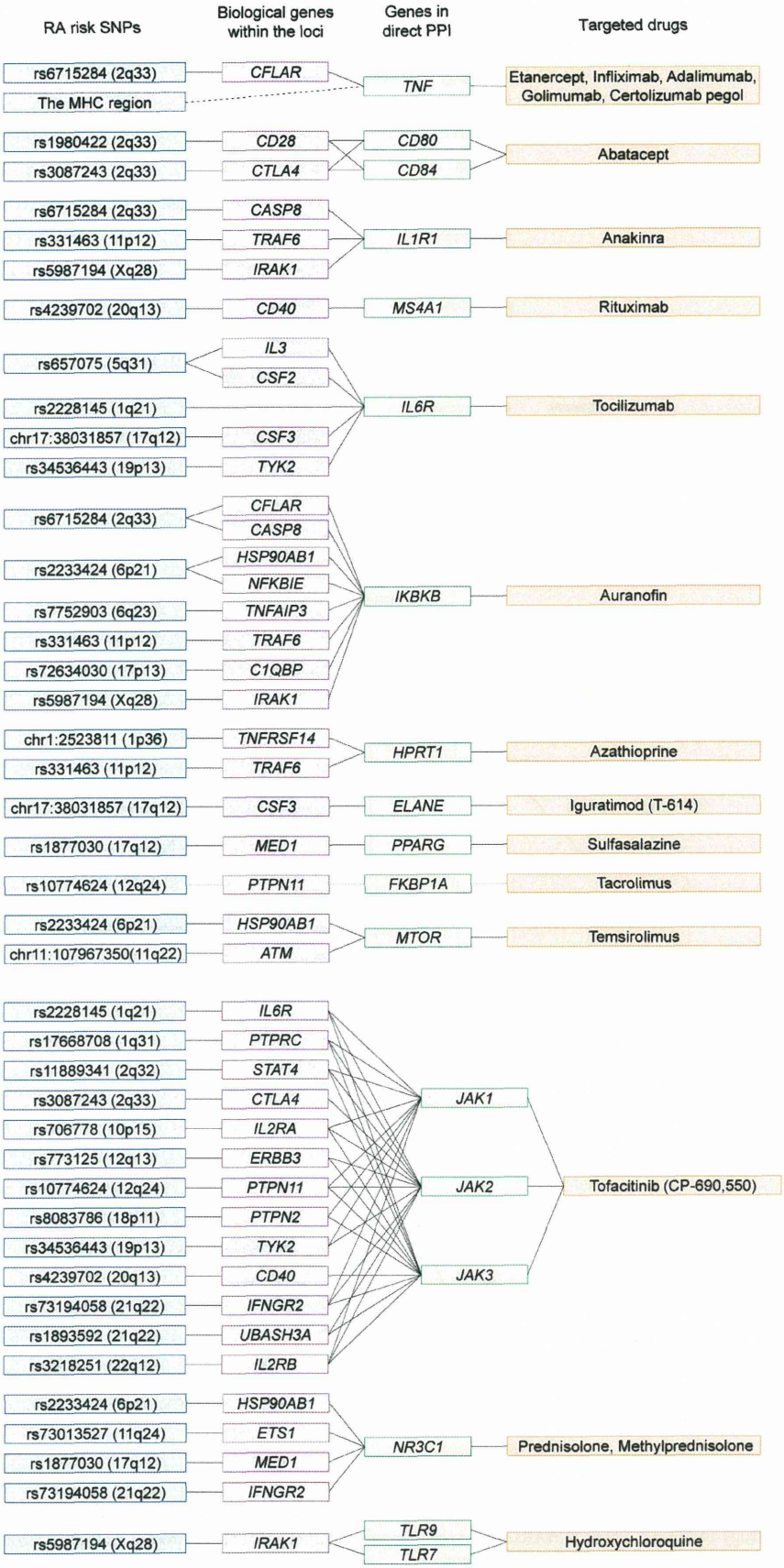

Extended Data Figure 8 | Connection between RA risk genes and approved RA drugs. Full lists of the connections between RA risk SNPs (blue boxes), biological candidate genes from each risk locus (purple boxes), genes from the expanded PPI network (green boxes) and approved RA drugs (orange boxes). Black lines indicate connections. Only *IL6R* is a direct connection between an SNP–biological gene–drug (tocilizumab)[19,20]; all other SNP–drug connections are through the PPI network.

Extended Data Table 1 | Characteristics of the study cohorts

a

Study stage	Cohort	Ethnicity	Geographical origin	No. subjects			RA case sero-positivity
				Cases	Controls	Total	
GWAS meta-analysis (Stage 1)	BRASS	European	North America	483	1,631	2,114	100% CCP+
	CANADA		Canada	589	1,554	2,143	100% CCP+
	EIRA		Sweden	1,097	1,044	2,141	100% CCP+
	NARAC1		North America	863	1,191	2,054	100% CCP+
	NARAC2		North America	896	6,603	7,499	100% CCP+
	WTCCC		United Kingdom	1,520	10,507	12,027	100% CCP+ or RF+
	RACI-UK		United Kingdom	1,645	6,082	7,727	100% CCP+
	RACI-US		North America	997	2,132	3,129	100% CCP+
	RACI-SE-E		Sweden	740	1,117	1,857	100% CCP+
	RACI-SE-U		Sweden	522	962	1,484	100% CCP+
	RACI-NL		Netherland	303	2,001	2,304	100% CCP+
	RACI-ES		Spain	397	399	796	100% CCP+
	RACI-i2b2		North America	882	1,863	2,745	100% CCP+
	ReAct		France	275	804	1,079	70% CCP+ or RF+
	Dutch (AMC, BeSt, LUMC, DREAM)		Netherland	1,172	1,684	2,856	80% CCP+ or RF+
	ACR-REF (BRAGGSS, BRAGGSS2, ERA, KI, TEAR)		North America & Europe	347	264	611	85% CCP+ or RF+
	CORRONA		North America	894	1,838	2,732	61% CCP+ or RF+, 32% unknown
	Vanderbilt		North America	739	2,247	2,986	31% CCP+ or RF+, 56% unknown
	GARNET (BioBank Japan Project; BBJ)	Asian	Japan	2,414	14,245	16,659	79% CCP+, 76% RF+
	GARNET (Kyoto University)		Japan	1,237	2,087	3,324	85% CCP+, 86% RF+
	GARNET (IORRA)		Japan	423	559	982	87% CCP+, 88% RF+
	Korea		Korea	799	751	1,550	100% CCP+
	European	-	-	14,361	43,923	58,284	-
	Asian	-	-	4,873	17,642	22,515	-
	Trans-ethnic	-	-	19,234	61,565	80,799	-
In-silico replication study (Stage 2)	Genentech	European	North America	2,780	4,700	7,480	44% CCP+, 52% unknown 81% RF+, 1.7% unknown
	China	Asian	China	928	835	1,763	48% CCP+
	Total	-	-	3,708	5,535	9,243	-
De-novo replication study (Stage 3)	CANADAII	European	Canada	995	1,101	2,096	100% CCP+
	GARNET	Asian	Japan	5,943	5,557	11,500	81% CCP+, 86% RF+
	Total	-	-	6,938	6,658	13,596	-
Total	European	-	-	18,136	49,724	67,860	-
	Asian	-	-	11,744	24,034	35,778	-
	Trans-ethnic	-	-	29,880	73,758	103,638	-

b

Study stage	Cohort	Genotyping platform	GWAS QC criteria				Imputation method			No.SNPs after QC		Inflation factor		Covariates	X chrom. data
			Sample call rate	SNP call rate	MAF	HWE P-value	Reference panel	MAF	Quality score	Genotyped	Imputed	λ_{GC}	λ_{GC_1000}		
GWAS meta-analysis (Stage 1)	BRASS	Affymetrix Genome-wide Human SNP Array 6.0	>0.95	>0.95	>0.01	$>10^{-6}$	1000 Genomes Phase I (α) Europeans	>0.005	>0.5	649,178	8,201,244	1.015	1.008	Top 5 PCs	Available
	CANADA	Illumina HumanCNV370-Duo BeadChip	>0.95	>0.95	>0.01	$>10^{-6}$	1000 Genomes Phase I (α) Europeans	>0.005	>0.5	295,430	7,933,623	1.002	1.001	Top 5 PCs	Available
	EIRA	HumanHap300 BeadChip	>0.95	>0.95	>0.01	$>10^{-6}$	1000 Genomes Phase I (α) Europeans	>0.005	>0.5	298,193	8,163,538	0.991	0.994	Top 5 PCs	N.A.
	NARAC1	Illumina HumanHap550 BeadChip	>0.95	>0.95	>0.01	$>10^{-6}$	1000 Genomes Phase I (α) Europeans	>0.005	>0.5	479,671	8,254,787	1.017	1.012	Top 5 PCs	N.A.
	NARAC2	HumanHap300 BeadChip	>0.95	>0.95	>0.01	$>10^{-6}$	1000 Genomes Phase I (α) Europeans	>0.005	>0.5	261,974	7,733,592	1.023	1.003	Top 5 PCs	N.A.
	WTCCC	Affymetrix Genome-wide Human SNP Array 5.0	>0.99	>0.99	>0.01	$>10^{-5}$	1000 Genomes Phase I (α) Europeans	>0.005	>0.5	339,790	7,385,370	1.043	1.004	Top 5 PCs	N.A.
	RACI-UK	Illumina Immunochip custom array	>0.99	>0.99	>0.01	$>10^{-6}$	1000 Genomes Phase I (α) Europeans	>0.005	>0.7	126,740	873,840	1.058	1.008	Top 10 PCs	Available
	RACI-US	Illumina Immunochip custom array	>0.99	>0.99	>0.01	$>10^{-6}$	1000 Genomes Phase I (α) Europeans	>0.005	>0.7	120,589	843,395	1.031	1.012	Top 10 PCs	Available
	RACI-SE-E	Illumina Immunochip custom array	>0.99	>0.99	>0.01	$>10^{-6}$	1000 Genomes Phase I (α) Europeans	>0.005	>0.7	124,801	870,585	1.003	1.002	Top 10 PCs	Available
	RACI-SE-U	Illumina Immunochip custom array	>0.99	>0.99	>0.01	$>10^{-6}$	1000 Genomes Phase I (α) Europeans	>0.005	>0.7	123,998	870,797	0.986	0.988	Top 10 PCs	Available
	RACI-NL	Illumina Immunochip custom array	>0.99	>0.99	>0.01	$>10^{-6}$	1000 Genomes Phase I (α) Europeans	>0.005	>0.7	124,480	862,815	1.109	1.051	Top 10 PCs	Available
	RACI-ES	Illumina Immunochip custom array	>0.99	>0.99	>0.01	$>10^{-6}$	1000 Genomes Phase I (α) Europeans	>0.005	>0.7	124,459	859,540	1.081	1.152	Top 10 PCs	Available
	RACI-i2b2	Illumina Immunochip custom array	>0.99	>0.99	>0.01	$>10^{-6}$	1000 Genomes Phase I (α) Europeans	>0.005	>0.7	118,731	829,507	1.003	1.001	Top 10 PCs	Available
	ReAct	Illumina OmniExpress BeadChip Illumina Human 660W-Quad BeadChip	>0.98	>0.99	>0.01	$>10^{-6}$	1000 Genomes Phase I (α) Europeans	>0.005	>0.5	257,299	7,588,538	0.992	0.991	Top 5 PCs	Available
	Dutch	Illumina Human 660W-Quad BeadChip Illumina HumanHap550 BeadChip Illumina HumanCNV370-Duo BeadChip	>0.95	>0.95	>0.01	$>10^{-6}$	1000 Genomes Phase I (α) Europeans	>0.005	>0.5	284,884	7,956,686	1.023	1.011	Top 5 PCs	Available
	ACR-REF	Illumina OmniExpress BeadChip Illumina Human 660W-Quad BeadChip	>0.95	>0.95	>0.01	$>10^{-6}$	1000 Genomes Phase I (α) Europeans	>0.005	>0.5	234,075	7,593,678	1.026	1.070	Top 5 PCs	Available
	CORRONA	Illumina OmniExpress BeadChip	>0.98	>0.99	>0.01	$>10^{-6}$	1000 Genomes Phase I (α) Europeans	>0.005	>0.5	552,896	8,400,238	1.001	1.000	Top 5 PCs	Available
	Vanderbilt	Illumina OmniExpress BeadChip	>0.98	>0.99	>0.01	$>10^{-6}$	1000 Genomes Phase I (α) Europeans	>0.005	>0.5	541,143	8,372,666	0.987	0.995	Top 5 PCs	Available
	BBJ	Illumina HumanHap610-Quad BeadChip	>0.98	>0.99	>0.01	$>10^{-7}$	1000 Genomes Phase I (α) Asians	>0.005	>0.5	477,784	6,874,738	1.038	1.002	-	Available
	Kyoto	Illumina HumaHap610-Quad BeadChip Illumina HumanHap550 BeadChip Illumina HumanCNV370-Duo BeadChip	>0.90	>0.95	>0.05	$>10^{-7}$	1000 Genomes Phase I (α) Asians	>0.005	>0.5	227,348	6,254,431	1.099	1.038	-	N.A.
	IORRA	Affymetrix Genome-wide Human SNP Array 6.0	>0.95	>0.98	>0.05	$>10^{-6}$	1000 Genomes Phase I (α) Asians	>0.005	>0.5	465,832	6,567,923	0.992	0.989	-	Available
	Korea	Illumina Human 660W-Quad BeadChip Illumina HumanHap550 BeadChip	>0.90	>0.90	>0.01	$>10^{-6}$	1000 Genomes Phase I (α) Asians	>0.005	>0.5	418,837	6,424,378	1.007	1.007	-	Available
	European	-	-	-	-	-	-	-	-	-	8,747,962	1.073	1.003	-	-
	Asian	-	-	-	-	-	-	-	-	-	6,619,871	1.041	1.005	-	-
	Trans-ethnic	-	-	-	-	-	-	-	-	-	9,739,303	1.072	1.002	-	-
In-silico replication study (Stage 2)	Genentech	Illumina HumanOmni1-Quad_v1-0_B Illumina Humanhap550K	>0.95	>0.95	>0.10	$>10^{-4}$	1000 Genomes Phase I (α) Europeans	>0.005	>0.5	-	-	-	-	Top 5 PCs	N.A.
	China	Affymetrix Genome-wide Human SNP Array 6.0	>0.95	>0.95	>0.05	$>10^{-3}$	1000 Genomes Phase I (α) Asians	>0.005	>0.5	-	-	-	-	Top 5 PCs	N.A.
De-novo replication study (Stage 3)	CANADAII	iPlex genotying system	-	-	-	-	-	-	-	-	-	-	-	-	Available
	GARNET	Taqman genotyping system	-	-	-	-	-	-	-	-	-	-	-	-	Available

a, Characteristics of the cohorts and subjects enrolled in the study. **b**, Genotype and imputation methods of the studies. CCP, anti-citrullinated peptide antibody; chrom, chromosome; N.A., not available; PC, principal component; QC, quality control; RF, rheumatoid factor.

Extended Data Table 2 | *cis*-eQTL of RA risk SNPs

a

RA risk SNP	Chr.	Position (bp)	eQTL gene	Cis-eQTL effect of best proxy SNP				Cis-eQTL effect of top eQTL SNP			
				Proxy SNP	Position (bp)	eQTL *P*	r^2	eQTL SNP	Position (bp)	eQTL *P*	r^2
chr1:2523811	1	2,523,811	*PLCH2*	rs10910099	2,533,552	2.2E-18	0.87	rs2494435	2,359,280	2.6E-45	<0.25
			TNFRSF14	rs2843401	2,528,133	1.1E-28	0.87	rs734999	2,513,216	2.1E-90	0.43
rs227163	1	7,961,206	*PARK7*	rs227163	7,961,206	4.6E-10	1.00	rs3766606	8,022,197	1.0E-53	<0.25
			MANEAL,YRDC	rs2306627	38,260,503	3.9E-09	0.84	rs2306426	36,451,618	7.7E-10	<0.25
rs28411352	1	38,278,579	*INPP5B*	rs2306627	38,260,503	7.5E-23	0.84	rs4072980	38,456,106	1.2E-113	<0.25
			SF3A3	rs2306627	38,260,503	3.3E-17	0.84	rs4072980	38,456,106	1.1E-190	<0.25
			FHL3	rs2306627	38,260,503	1.1E-11	0.84	rs4634868	38,465,315	9.8E-198	<0.25
rs2476601	1	114,377,568	*PTPN22*	rs2476601	114,377,568	3.4E-10	1.00	rs7555634	114,367,116	5.3E-43	<0.25
			AQP10	rs6684439	154,395,839	3.3E-06	0.89	rs6668968	154,293,675	3.8E-40	<0.25
rs2228145	1	154,426,970	*IL6R*	rs4129267	154,426,264	3.2E-27	1.00	rs4537545	154,418,879	2.0E-29	0.96
			UBE2Q1	rs4129267	154,426,264	9.7E-08	1.00	rs6660775	154,538,554	3.9E-21	<0.25
rs2317230	1	157,674,997	*FCRL5*	rs3761959	157,669,278	1.7E-09	0.87	rs6427386	157,530,097	9.8E-198	<0.25
			FCRL3	rs7528684	157,670,816	9.8E-198	0.87	rs2210913	157,668,993	9.8E-198	0.87
rs4656942	1	160,831,048	*LY9*	rs4656942	160,831,048	2.7E-96	1.00	rs576334	160,797,514	5.8E-195	<0.25
rs72717009	1	161,405,053	*SDHC*	rs12731669	161,410,458	5.5E-05	0.97	rs16832871	161,335,758	1.4E-142	<0.25
			FCGR2B	rs12731669	161,410,458	4.2E-83	0.97	rs6674499	161,618,151	9.8E-198	<0.25
rs17668708	1	198,640,488	*PTPRC*	rs17669032	198,653,174	5.2E-05	0.97	rs2296618	198,666,232	2.1E-05	0.78
rs1980422	2	204,610,396	*CD28*	rs1980421	204,610,004	7.3E-18	1.00	rs2140148	204,572,140	8.1E-21	0.47
rs10028001	4	79,502,972	*ANXA3*	rs10028001	79,502,972	1.1E-04	1.00	rs4975144	79,474,040	1.4E-09	<0.25
rs2561477	5	102,608,924	*PAM*	rs411648	102,602,902	2.2E-113	1.00	rs2431321	102,118,794	9.8E-198	<0.25
			GIN1	rs2288786	102,600,754	1.3E-06	1.00	rs42431	102,400,063	2.6E-13	0.43
rs657075	5	131,430,118	*ACSL6*	rs657075	131,430,118	3.8E-12	1.00	rs253946	131,330,461	9.2E-26	0.32
chr6:14103212	6	14,103,212	*CD83*	rs12530098	14,107,197	2.6E-24	1.00	rs16874672	14,087,484	2.2E-26	0.90
			KCTD20	rs4713969	36,349,008	8.2E-05	0.99	rs4711453	36,439,391	3.1E-32	<0.25
rs2234067	6	36,355,654	*STK38*	rs4713969	36,349,008	1.4E-06	0.99	rs1812018	36,557,976	6.8E-15	<0.25
			-	rs4713969	36,349,008	2.1E-26	0.99	rs10947614	36,573,822	1.1E-146	<0.25
			SFRS3	rs4713969	36,349,008	2.6E-11	0.99	rs7743396	36,579,252	1.5E-52	<0.25
rs9373594	6	149,834,574	*C6orf72*	rs9377224	149,853,707	4.0E-06	1.00	rs9322189	149,909,933	1.8E-15	0.30
			NUP43	rs9377224	149,853,707	4.1E-64	1.00	rs9688350	150,052,113	9.8E-198	0.27
rs2451258	6	159,506,600	*RSPH3*	rs2485363	159,506,121	5.0E-05	1.00	rs12216499	159,368,524	2.0E-119	<0.25
rs1571878	6	167,540,842	*RNASET2*	rs1571878	167,540,842	9.8E-198	1.00	rs429083	167,383,972	9.8E-198	0.39
			TNPO3	rs3807306	128,580,680	1.4E-150	0.81	rs3807306	128,580,680	1.4E-150	0.81
chr7:128580042	7	128,580,042	-	rs3807306	128,580,680	2.4E-32	0.81	rs10229001	128,599,397	4.5E-49	0.48
			IRF5	rs3807306	128,580,680	9.8E-198	0.81	rs7807018	128,640,188	9.8E-198	0.48
rs2736337	8	11,341,880	*C8orf13.C8orf12*	rs2736340	11,343,973	1.6E-174	0.99	rs4840568	11,351,019	3.8E-175	0.92
			BLK	rs1478901	11,347,833	1.8E-120	0.99	rs998683	11,353,000	1.5E-120	0.95
			TRAF1	rs10985070	123,636,121	3.9E-72	1.00	rs2416804	123,676,396	3.8E-73	0.96
rs10985070	9	123,636,121	*PHF19*	rs10985070	123,636,121	2.9E-10	1.00	rs10760129	123,700,183	2.2E-10	0.95
			C5	rs10985070	123,636,121	4.9E-68	1.00	rs2416811	123,789,634	2.0E-146	0.31
rs947474	10	6,390,450	-	rs947474	6,390,450	6.5E-06	1.00	rs12416248	6,391,031	1.1E-43	<0.25
rs2671692	10	50,097,819	*WDFY4*	rs2671692	50,097,819	3.0E-09	1.00	rs7072606	49,933,974	1.1E-50	<0.25
			C11orf10	rs968567	61,595,564	3.1E-39	1.00	rs174538	61,560,081	2.5E-67	0.40
rs968567	11	61,595,564	*FADS1*	rs968567	61,595,564	8.1E-62	1.00	rs968567	61,595,564	8.1E-62	1.00
			FADS2	rs968567	61,595,564	4.8E-34	1.00	rs968567	61,595,564	4.8E-34	1.00
rs10774624	12	111,833,788	*SH2B3*	rs653178	112,007,756	1.7E-19	0.86	rs2239195	111,681,309	1.0E-33	<0.25
			ALDH2	rs653178	112,007,756	8.7E-07	0.86	rs16941669	112,245,637	4.4E-50	<0.25
rs4780401	16	11,839,326	*TXNDC11*	rs11075010	11,826,013	8.3E-09	0.93	rs12919035	11,821,508	4.4E-12	0.49
			ZNF594	rs8080217	5,164,761	8.7E-11	0.88	rs2071455	5,031,946	1.5E-12	0.65
rs72634030	17	5,272,580	*C17orf87*	rs8080217	5,164,761	3.3E-05	0.88	rs2641232	5,087,602	1.4E-53	<0.25
			-	rs8080217	5,164,761	3.6E-70	0.88	rs7426	5,288,983	9.8E-198	<0.25
			NUP88	rs8080217	5,164,761	3.3E-27	0.88	rs1989946	5,313,152	8.9E-96	<0.25
			MIS12	rs8080217	5,164,761	8.5E-10	0.88	rs1805448	5,384,327	2.2E-35	<0.25
			FBXL20	rs12937013	37,665,571	3.4E-15	1.00	rs8076462	37,400,025	3.1E-42	<0.25
rs1877030	17	37,740,161	*PPP1R1B*	rs1877030	37,740,161	1.8E-10	1.00	rs879606	37,781,849	8.0E-18	0.41
			-	rs11657058	37,699,378	3.9E-05	1.00	rs7219814	37,478,801	2.1E-111	<0.25
			IKZF3	rs4795385	37,733,148	8.8E-24	1.00	rs2517955	37,843,681	5.2E-82	0.33
			-	rs907092	37,922,259	6.6E-11	0.90	rs7219814	37,478,801	2.1E-111	<0.25
chr17:38031857	17	38,031,857	*IKZF3*	rs11557467	38,028,634	3.3E-05	0.84	rs9896940	37,895,975	3.1E-25	<0.25
			GSDMB	rs10852936	38,031,714	9.8E-198	0.98	rs9901146	38,043,343	9.8E-198	0.84
			ORMDL3	rs10852936	38,031,714	9.8E-198	0.98	rs8076131	38,080,912	9.8E-198	0.86
rs2469434	18	67,544,046	*CD226*	rs1610555	67,543,147	2.3E-33	0.99	rs763361	67,531,642	2.4E-50	0.66
rs4239702	20	44,749,251	*CD40*	rs4239702	44,749,251	1.3E-34	1.00	rs745307	44,747,086	1.5E-72	<0.25
			IL10RB	rs11702844	34,759,876	1.3E-11	0.97	rs1058867	34,669,381	3.0E-69	<0.25
rs73194058	21	34,764,288	*IFNAR1*	rs11702844	34,759,876	8.0E-12	0.97	rs2257167	34,715,699	4.2E-73	<0.25
			TMEM50B	rs11702844	34,759,876	3.1E-11	0.97	rs1059293	34,809,693	2.2E-103	<0.25
			-	rs11702844	34,759,876	2.8E-34	0.97	rs2834217	34,822,150	9.8E-198	<0.25
rs1893592	21	43,855,067	*UBASH3A*	rs1893592	43,855,067	6.4E-92	1.00	rs1893592	43,855,067	6.4E-92	1.00
rs2236668	21	45,650,009	*ICOSLG*	rs7278940	45,648,992	3.7E-06	1.00	rs3788111	45,668,171	8.4E-16	<0.25
rs11089637	22	21,979,096	-	rs11089637	21,979,096	9.8E-198	1.00	rs5754217	21,939,675	9.8E-198	0.87
			SYNGR1	rs909685	39,747,671	1.0E-140	1.00	rs909685	39,747,671	1.0E-140	1.00
rs909685	22	39,747,671	*MAP3K7IP1*	rs909685	39,747,671	1.3E-05	1.00	rs5750824	39,830,123	5.9E-07	0.28

b

SNP	Chr.	Position (bp)	eQTL gene	Nominal *P* for cis-eQTL	
				$CD4^+$ T-cell	$CD14^+16^-$ Monocyte
rs28411352	1	38,278,579	*INPP5B*	0.022	**3.6E-16**
			FHL3	0.081	**8.9E-13**
rs2317230	1	157,674,997	*FCRL3*	**3.5E-06**	0.87
rs9653442	2	100,825,367	*AFF3*	**5.2E-08**	0.18
rs7731626	5	55,444,683	*IL6ST*	**2.3E-07**	0.0087
			ANKRD55	**4.1E-14**	0.43
rs2234067	6	36,355,654	*ETV7*	2.9E-04	**1.1E-10**
rs9373594	6	149,834,574	*NUP43*	5.4E-04	**1.5E-05**
rs1571878	6	167,540,842	*RNASET2*	**6.9E-20**	**1.3E-05**
rs67250450	7	28,174,986	*JAZF1*	**3.6E-17**	2.0E-04
chr7:128580042*	7	128,580,042	*TNPO3*	1.0E-04	**3.0E-07**
			MEGF9	**3.3E-06**	0.10
rs10985070	9	123,636,121	*PSMD5*	0.017	**1.8E-05**
			PHF19	0.0016	**5.6E-06**
rs968567	11	61,595,564	*FADS2*	**1.4E-31**	**8.9E-35**
			FADS1	**2.1E-32**	0.094
rs11605042	11	72,411,664	*STARD10*	0.82	**1.0E-07**
rs4409785	11	95,311,422	*SESN3*	**1.5E-11**	0.43
rs773125	12	56,394,954	*SUOX*	0.27	**1.1E-09**
rs1633360	12	58,108,052	*TSPAN31*	0.13	**1.0E-05**
			METTL21B	**1.4E-09**	**4.0E-10**
rs9603616	13	40,368,069	*COG6*	0.0011	**1.2E-05**
rs4780401	16	11,839,326	*TXNDC11*	**1.3E-05**	0.62
rs72634030	17	5,272,580	*MIS12*	0.0039	**1.3E-05**
rs1877030	17	37,740,161	*STARD3*	0.048	**4.5E-05**
			GSDMA	**2.1E-06**	0.63
chr17:38031857†	17	38,031,857	*GSDMB*	**4.3E-11**	0.19
			ORMDL3	**6.8E-09**	0.0098
rs4239702	20	44,749,251	*CD40*	0.31	**1.7E-08**
rs73194058	21	34,764,288	*IFNGR2*	0.096	**1.9E-06**
			TMEM50B	**7.5E-07**	0.013
rs1893592	21	43,855,067	*UBASH3A*	**3.8E-14**	0.92

a, *cis*-eQTL of PBMCs in the RA risk SNPs. Significant *cis*-eQTLs of RA risk SNPs is indicated (FDR $q < 0.05$). SNPs and positions are based on the positive strand of NCBI build 37. Linkage disequilibrium of the proxy SNPs evaluated in the eQTL study and the best *cis*-eQTL SNP in the region with the RA risk SNPs is indicated as r^2 values. When the expression probe was not assigned to any genes, the eQTL gene is labelled with a dash. **b**, *cis*-eQTL of T cells and monocytes in the RA risk SNPs. Significant *cis*-eQTLs of RA risk SNPs are indicated in bold (gene-based permutation $P < 0.05$).

* *cis*-eQTL of the proxy SNP (rs3807307, $r^2 = 0.96$) was evaluated.

† *cis*-eQTL of the proxy SNP (rs11557466, $r^2 = 0.98$) was evaluated.

The Journal of
Rheumatology

The Journal of Rheumatology Volume 41, no. 2

A Clinical, Pathological, and Genetic Characterization of Methotrexate-associated Lymphoproliferative Disorders

Noriyuki Yamakawa, Masakazu Fujimoto, Daisuke Kawabata, Chikashi Terao, Momoko Nishikori, Ran Nakashima, Yoshitaka Imura, Naoichiro Yukawa, Hajime Yoshifuji, Koichiro Ohmura, Takao Fujii, Toshiyuki Kitano, Tadakazu Kondo, Kimiko Yurugi, Yasuo Miura, Taira Maekawa, Hiroh Saji, Akifumi Takaori-Kondo, Fumihiko Matsuda, Hironori Haga and Tsuneyo Mimori

J Rheumatol 2014;41;293-299
http://www.jrheum.org/content/41/2/293

A Clinical, Pathological, and Genetic Characterization of Methotrexate-associated Lymphoproliferative Disorders

Noriyuki Yamakawa, Masakazu Fujimoto, Daisuke Kawabata, Chikashi Terao, Momoko Nishikori, Ran Nakashima, Yoshitaka Imura, Naoichiro Yukawa, Hajime Yoshifuji, Koichiro Ohmura, Takao Fujii, Toshiyuki Kitano, Tadakazu Kondo, Kimiko Yurugi, Yasuo Miura, Taira Maekawa, Hiroh Saji, Akifumi Takaori-Kondo, Fumihiko Matsuda, Hironori Haga, and Tsuneyo Mimori

ABSTRACT. ***Objective.*** Methotrexate-associated lymphoproliferative disorders (MTX-LPD) often regress spontaneously during MTX withdrawal, but the prognostic factors remain unclear. The aim of our study was to clarify the clinical, histological, and genetic factors that predict outcomes in patients with MTX-LPD.

Methods. Patients with MTX-LPD diagnosed between 2000 and 2012 were analyzed retrospectively regarding their clinical course, site of biopsy, histological typing, Epstein-Barr virus (EBV) *in situ* hybridization and immunostaining, and HLA type.

Results. Twenty-one patients, including 20 with rheumatoid arthritis (RA) and 1 with polymyositis, were analyzed. The mean dose of MTX was 6.1 mg/week and the mean duration of treatment was 71.1 months. Clinically, 5 patients were diagnosed with EBV-positive mucocutaneous ulcer (EBVMCU) and had polymorphic histological findings. The proportion of those patients successfully treated solely by withdrawal of MTX was significantly greater than that of those without EBVMCU (75% vs 7.7%, p = 0.015). The HLA-B15:11 haplotype was more frequent in patients with EBV+ RA with MTX-LPD than in healthy Japanese controls (p = 0.0079, Bonferroni's method). EBV latency classification and HLA typing were not associated with the prognosis of MTX-LPD in our cohort.

Conclusion. Our data demonstrate that patients in the EBVMCU, a specific clinical subgroup of MTX-LPD, had a better clinical outcome when MTX was withdrawn than did other patients with MTX-LPD. (First Release Dec 15 2013; J Rheumatol 2014;41:293–9; doi:10.3899/jrheum.130270)

Key Indexing Terms:
RHEUMATIC DISEASES | RHEUMATOID ARTHRITIS
SKIN MANIFESTATIONS | HLA ANTIGENS | HEMATOPOIETIC SYSTEM

Methotrexate (MTX)-associated lymphoproliferative disorders (LPD) are a lymphoid proliferation or lymphoma that occur in patients immunosuppressed with MTX, classified as a part of the "other iatrogenic immunodeficiency-associated lymphoproliferative disorders" category by the World Health Organization (WHO) in 2008[1]. Because MTX has recently gained acceptance as a first-line therapy for rheumatoid arthritis (RA)[2,3] and other systemic

From the Department of Rheumatology and Clinical Immunology, the Department of Diagnostic Pathology, the Center for Genomic Medicine, and the Department of Hematology and Oncology, Kyoto University Graduate School of Medicine; the Department of Transfusion Medicine and Cell Therapy, Kyoto University Hospital; the HLA Foundation Laboratory, Kyoto, Japan.

N. Yamakawa, MD, Department of Rheumatology and Clinical Immunology; M. Fujimoto, MD, the Department of Diagnostic Pathology; D. Kawabata, MD, PhD, Department of Rheumatology and Clinical Immunology; C. Terao, MD, PhD, Department of Rheumatology and Clinical Immunology, and the Center for Genomic Medicine; M. Nishikori, MD, PhD, Department of Hematology and Oncology; R. Nakashima, MD, PhD; Y. Imura, MD, PhD; N. Yukawa, MD, PhD; H. Yoshifuji, MD, PhD; K. Ohmura, MD, PhD; T. Fujii, MD, PhD, Department of Rheumatology and Clinical Immunology; T. Kitano, MD; T. Kondo, MD, PhD, Department of Hematology and Oncology, Kyoto University Graduate School of Medicine; K. Yurugi; Y. Miura, MD, PhD; T. Maekawa, MD, PhD, Department of Transfusion Medicine and Cell Therapy, Kyoto University Hospital; H. Saji, BSc, HLA Foundation Laboratory; A. Takaori-Kondo, MD, PhD, Department of Hematology and Oncology; F. Matsuda, MD, PhD, Center for Genomic Medicine; H. Haga, MD, PhD, Department of Diagnostic Pathology; T. Mimori, MD, PhD, Department of Rheumatology and Clinical Immunology, Kyoto University Graduate School of Medicine.

Address correspondence to Dr. D. Kawabata, Kyoto University, Department of Rheumatology and Clinical Immunology, Shogoin-Kawahara-cho, 54 Sakyo-ku, Kyoto 606-8507, Japan. E-mail: yakugo@gmail.com

Accepted for publication October 8, 2013.

rheumatic diseases (SRD), the incidence of MTX-LPD is expected to increase. A better understanding of this important disease is somewhat limited by its rarity. Epstein-Barr virus (EBV) infection is thought to play an important role in the pathogenesis of MTX-LPD, although EBV can only be detected on histopathologic examination in about half the cases of MTX-LPD[4].

Under normal circumstances, EBV-specific cytotoxic T lymphocytes (EBV-CTL) act to suppress EBV-infected B cells. However, if the function of EBV-CTL is impaired by immunosuppressants, such as MTX or by aging, EBV-infected B cells are reactivated to induce B cell proliferation, leading to the development of LPD. There is speculation that MTX could reactivate latent EBV infection, because patients with SRD treated with regimens that include MTX have higher mean EBV loads in their blood than those who do not[5]. EBV-related LPD (EBV-LPD) can be categorized into 3 types on the basis of their expression of EBV-encoded small RNA (EBER), EBV latent membrane protein-1 (LMP1), and EBV nuclear antigen-2 (EBNA2): latency I (EBER+, LMP-1–, EBNA2–) as seen in Burkitt's lymphoma; latency II (EBER+, LMP-1+, EBNA-2–) as seen in Hodgkin's lymphoma or nasopharyngeal carcinoma; and latency III (EBER+, LMP-1+, EBNA-2+) as seen in posttransplant LPD (PT-LPD)[6]. EBV-LPD frequently occurs in immunosuppressed patients and its prognosis appears to vary widely.

LPD with EBV-positive mucocutaneous ulcer (EBVMCU) has been reported as a distinct disease entity with a self-limiting and indolent clinical course[7]. EBVMCU is found in various conditions of immunosuppression, including MTX-LPD or in age-related immunosenescence. The latter is characterized by age-related EBV+ B cell LPD (Age-LPD) on a background of EBV infection in elderly patients without immunodeficiency[8]. Although MTX-LPD often shows spontaneous regression, it is not clear whether MTX-LPD with EBVMCU has a better prognosis. The aim of our study was to clarify the clinical, histological, and genetic factors predictive of a good prognosis in patients with MTX-LPD.

MATERIALS AND METHODS

Patients. Twenty-one patients with SRD who developed MTX-LPD between 2000 and 2012 were included in our study. There were 20 with RA and 1 with polymyositis (PM). Of the 20 patients with RA, 3 had RA overlapping with Sjögren syndrome (SS), 1 had RA with systemic lupus erythematosus (SLE), and 1 had RA with polymyalgia rheumatica (PMR). The diagnoses of RA, PM, SS, SLE, and PMR were made according to the American College of Rheumatology classification criteria. The stage of RA was evaluated by Steinbrocker's classification and the stage of LPD by Ann Arbor classification. After the histologic diagnosis of MTX-LPD was made, MTX was withdrawn in all patients. Necessity of chemotherapy was determined according to the histology, karyotypes, stages, or clinical judgment of poor response to MTX withdrawal.

Ethics statement. The study was conducted in compliance with the Declaration of Helsinki and was approved by the Kyoto University Ethics Committee Review Board; written informed consent was obtained from all patients.

Histological analysis. Two pathologists performed histological analysis of specimens from each patient. Diagnoses were made in accordance with the criteria specified in *WHO Tumors of Hematopoietic and Lymphoid Tissues*, fourth edition[1]. Immunostaining of paraffin sections was performed using monoclonal antibodies against LMP1 (Clone CS.1-4, Dako) and EBNA2 (M7004, PE2, Dako). The presence of EBER was determined by *in situ* hybridization (ISH) using a peptide nucleic acid (PNA) ISH detection kit (K5201, Dako) and an EBER PNA Probe/Fluorescein kit (Y5200, Dako).

Typing of HLA. HLA-A, B, and DR typing studies of 16 cases of RA with MTX-LPD and 96 control cases of RA without MTX-LPD diagnosed in our department were undertaken using the PCR-Luminex method. The frequency of each HLA allele was analyzed with reference to the Japanese HLA laboratory database (http://hla.or.jp/haplo/haplonavi.php?type=haplo&lang=ja), which includes over 20,000 cases.

Statistical analysis. Data are expressed as mean ± SD. Comparisons of HLA and histological data were made using Fisher's exact test. Each allele seen in more than 2 cases was assessed with significant level corrected p value (Pc) by Bonferroni's method. A Kaplan-Meier plot of the chemotherapy-free survival was evaluated by the log-rank test. All analyses were performed using PASW Statistics 18 (18.0.0) and statistical significance was defined as $p < 0.05$.

RESULTS

Clinical and pathological details of patients with MTX-LPD. The clinical, pathological, and genetic characteristics of 21 cases of MTX-LPD are shown in Table 1; 17 (81%) were female; the mean age was 65.8 ± 7.5 years (range 52 to 79 yrs). The average dose of MTX was 6.1 ± 1.7 mg/week; treatment duration was 71.1 ± 57.8 months. Staging of RA was undertaken using Steinbrocker's classification; 1 patient fulfilled the criteria for stage I, 3 for stage II, 3 for stage III, and 13 for stage IV. Three patients (cases 1, 5, and 15) were treated with infliximab. Seventeen out of 20 RA cases (85%) were rheumatoid factor (RF)-positive and 7 out of 14 cases (50%) were anticitrullinated protein antibody (ACPA)-positive.

The pathological findings were as follows: 10 cases were diagnosed with diffuse large B cell lymphoma (DLBCL), 7 with polymorphic lymphoproliferative disorder (p-LPD), 3 with HL, and 1 with small B cell lymphoma that later transformed into DLBCL. The biopsy site was extranodal in 12 cases (57%); all 7 cases of p-LPD were extranodal, while 3 cases of HL were nodal. Of the 10 cases of DLBCL, half were extranodal and half nodal. Twelve out of 20 cases (60%) were EBER-positive, while 8 cases of 19 (42%) were LMP1-positive and 3 cases out of 19 (16%) were EBNA2-positive. EBV latency was classified by means of EBER, LMP1, and EBNA2 expression into 4 groups: EBV-negative and latencies I–III. Representative histological images are shown in Figure 1. The cases diagnosed as p-LPD comprised 7 of the 12 patients in latency I–III groups; but there were none among the 8 patients in the EBV-negative group ($p = 0.012$). Extranodal involvement was found in 8 of 12 patients in the latency I–III groups but only 3 of 8 in the EBV-negative group. EBVMCU was diagnosed in 5 cases (cases 1, 2, 4, 5, and 21), each charac-

Table 1. Clinical and pathological findings in 21 cases of methotrexate-associated lymphoproliferative disorders (MTX-LPD).

No.	Age	Sex	Disease	Dose of MTX, mg/week	Duration of MTX, mos	E/N	Site of Biopsy	Histology	EBER	LMP1	EBNA2	EBV Latency	LPD Stage	IPI	Therapy and Response	Response (final state)	Prognosis	Followup period, mos
1	76	F	RA	8.0	27	E(MCU)	left eyelid	p-LPD	(+)	(+)	(+)	III	I	L	W → CR	CR	A	24
2	64	F	RA	8.0	120	E(MCU)	buccal mucosa	p-LPD	(+)	(+)	(+)	III	IV	HI	W	ND	D#1	1
3	71	F	RA	8.0	184	E	left latero-abdominal nodule	p-LPD	(+)	(+)	(+)	III	IV	H	R-CHOP → PR → oral VP-16 → CR	CR	A	31
4	59	F	RA	5.0	63	E(MCU)	left eyelid	p-PLD	(+)	(+)	(–)	II	I	H	W→ CR	CR	A	37
5	61	F	RA	10.0	74	E(MCU)	right lower leg ulcer	p-PLD	(+)	(+)	(–)	II	IV	H	R-CHOP → CR	CR	A	25
6	65	F	RA SS	4.0	27	N	left axillary lymph node	HL	(+)	(+)	(–)	II	II	LI	W → CR → relapse → ABVD, C-MOPP → PR → RT → CR	CR	A	79
7	65	F	RA	5.0	66	N	right axillary lymph node	HL	(+)	(+)	(–)	II	IV	HI	W → CR → relapse → ABVD → CR	CR	D#2	17
8	58	F	RA	4.0	66	N	inguinal lymph node	SBL	(+)	(+)	(–)	II	II	L	CHOP, RT → CR → relapse → observe → R-ICE, CHASER, auto-PBSCT (MEAM) → CR	CR	D#3	92
9	67	F	RA SS	6.0	16	E	parotid gland	DLBCL	(+)	(–)	(–)	I	III	H	R-CHOP → CR → relapse → R-DeVIC → PR → RT, CHASER, R-ESHAP, mini-MEAM, GEM, CPT-11 → PD	PD	D	90
10	61	F	RA	6.0	193	N	right cervical lymph node	DLBCL	(+)	(–)	(–)	I	III	LI	R-CHOP → CR	CR	A	45
11	79	M	RA	8.0	169	E	right forearm	p-LPD	(+)	(–)	(–)	I	I	LI	W → CR	CR	A	9
12	66	M	RA	6.0	46	N	left submandibular lymph node	DLBCL	(–)	(–)	(–)	n	IV	HI	R → CR → relapse → CHOP → PD	PD	D	27
13	72	F	RA SLE	6.0	ND	N	right submandibular lymph node	DLBCL	(–)	(–)	(–)	n	II	LI	R-CHOP → CR → relapse → R-DeVIC	PD	A	48
14	74	F	RA	7.0	74	N	right cervical lymph node	DLBCL	(–)	(–)	(–)	n	II	LI	W → CR	CR	A	32
15	52	F	RA SS	5.0	47	E	precordial skin	DLBCL	(–)	(–)	(–)	n	IV	HI	R-CHOP → CR	CR	A	84
16	76	M	RA	4.0	ND	N	right axillary lymph node	HL	(–)	(–)	(–)	n	III	HI	W	ND	A	1
17	71	M	RA PMR	5.0	7	N	right cervical lymph node	DLBCL	(–)	(–)	(–)	n	II	HI	R-CHOP → PR	PR	A	8
18	62	F	RA	8.0	21	E	right orbital fossa	DLBCL	(–)	(–)	(–)	n	II	LI	R-CHOP → CR	CR	A	15
19	56	F	RA	5.5	98	E	left submandibular skin	DLBCL	(–)	(–)	(–)	n	II	L	W → CR	CR	A	14
20	71	F	RA	6.0	48	E	lumbar mass	DLBCL	NE	NE	NE	ND	II	LI	R-CHOP, RT → CR	CR	A	132
21	56	F	PM	4.0	4	E(MCU)	left lower leg ulcer	p-LPD	(+)	NE	NE	ND	I	L	W → CR	CR	A	33

No. 1: Died soon from intercurrent disease (myelitis and sepsis). No. 2: Died from bleomycin-induced interstitial pneumonia. No. 3: died from pneumocystis pneumonia. PM: polymyositis; RA: rheumatoid arthritis; SS: Sjögren syndrome; SLE: systemic lupus erythematosus, PMR: polymyalgia rheumatica; E: extranodal; MCU: mucocutaneous ulcer lesion; N: nodal; EBV: Epstein-Barr virus; DLBCL: diffuse large B cell lymphoma; EBER: EBV-encoded small RNA; p-LPD: polymorphic lymphoproliferative disorder; SBL: small B cell lymphoma; HL: Hodgkin lymphoma; n: EBV-negative; NE: not examined; ND: not determined; IPI: international prognostic index; L: low risk; LI: low-intermediate risk; HI: high-intermediate risk; H: high risk; W: withdrawal of MTX only; R-CHOP: rituximab, cyclophosphamide, hydroxydaunorubicin, vincristine and prednisolone; ABVD: adriamycin, bleomycin, vinblastine and dacarbazine; C-MOPP: cyclophosphamide, vincristine, prednisolone and procarbazine; RT: radiotherapy; R-ICE: rituximab, ifosfamide, carboplatin and etoposide; MEAM: ranimustine (MCNU), etoposide, cytarabine and melphalan; R-DeVIC: rituximab, dexamethasone, etoposide, ifosfamide and carboplatin; R-ESHAP: rituximab, etoposide, prednisolone, high-dose cytarabine and cisplatin; GEM: gemcitabine; CPT-11: irinotecan; CR: complete remission; PD: progressive disease; PR: partial remission; A: alive; D: dead; auto-PBSCT: autologous peripheral blood stem cell transplantation; CHASER: cyclophosphamide, cytarabine, dexamethasone, etoposide, and rituximab

terized by sharply demarcated skin ulcers with an erythematous appearance accompanied by crusting and necrosis (Figure 2) which, on histological examination, were found to be polymorphic with a mixture of lymphocytes and immunoblasts. Lymphocytic vasculitis was seen in 3 out of 5 cases (cases 2, 5, and 21). Four out of 5 cases (80%) of EBVMCU were seropositive.

HLA typing of patients with MTX-LPD. As shown in Table 2, we found that 3 cases out of 16 were heterozygous for the HLA-B15:11 allele. The allele frequency of HLA-B15:11

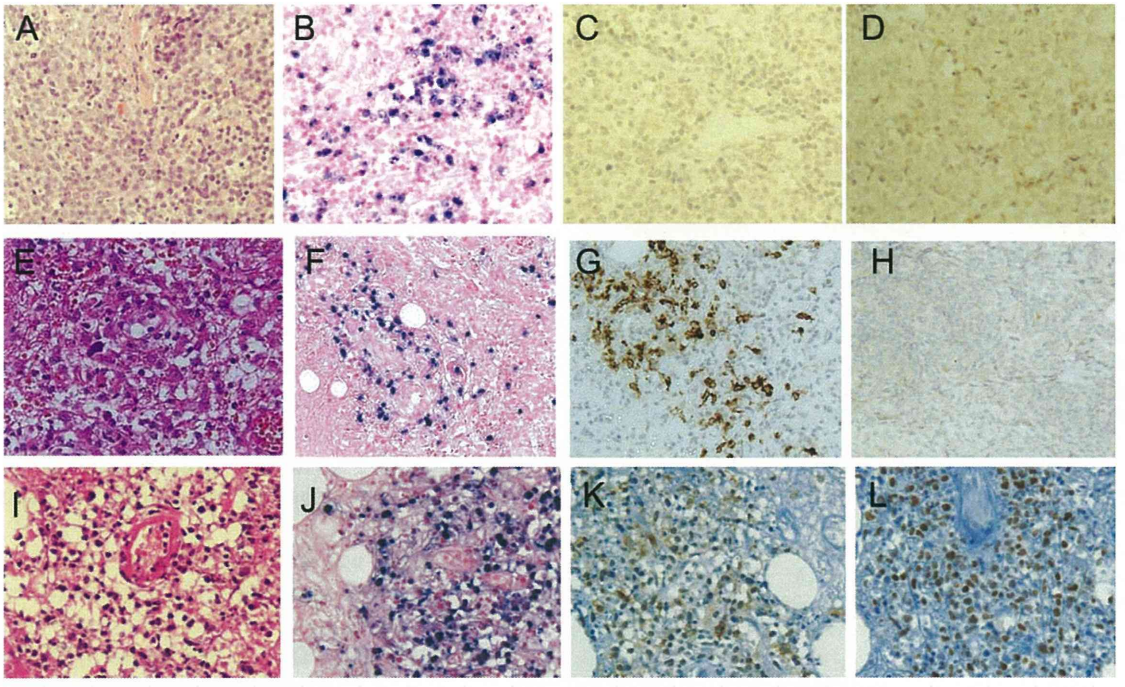

Figure 1. Pathological findings in 3 cases of MTX-LPD classified by EBV latency. A-D. DLBCL (case 10, latency I). E-H. Polymorphic LPD (case 4, latency II). I-L. Polymorphic LPD (case 3, latency III). Pathological findings are shown by H&E (A, E, I), EBER (B: positive, F: positive, J: positive), LMP1 (C: negative, G: positive, K: positive), and EBNA2 (D: negative, H: negative, L: positive) staining. MTX-LPD: methotrexate-associated lymphoproliferative disorders; EBV: Epstein-Barr virus; DLBCL: diffuse large B cell lymphoma; EBER: EBV-encoded small RNA; LMP1: EBV latent membrane protein-1; EBNA2: EBV nuclear antigen-2.

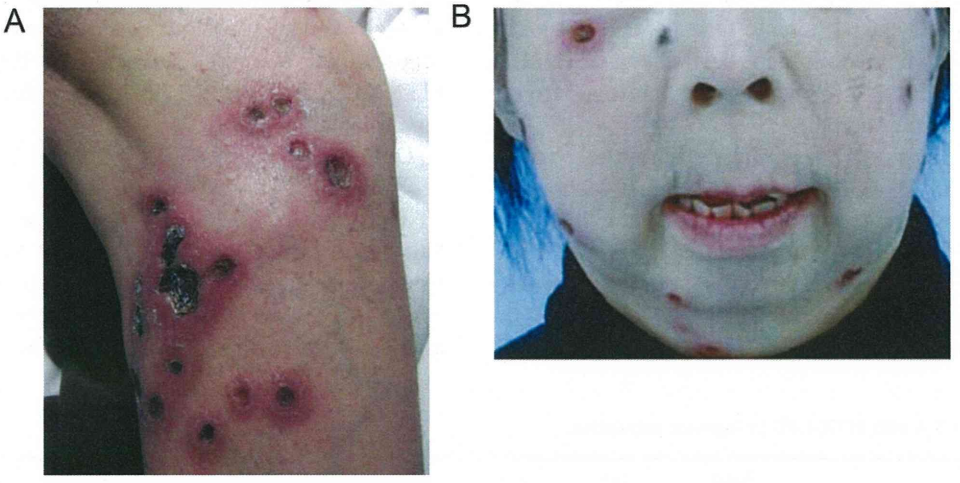

Figure 2. Two representative cases with skin manifestations of EBV-positive mucocutaneous ulcer (EBVMCU). Typical skin manifestations of EBVMCU (A: case 5, B: case 2) are shown. Characteristic sharply demarcated skin ulcers with an erythematous appearance accompanied by crusting and necrosis can be seen.

was higher in EBV+ RA with MTX-LPD, compared with the control JHD group and that of the Japanese RA cohort (Pc = 0.0079 and 0.024, respectively, Table 3). RA-shared epitopes were observed in 11 of 16 cases (69%), a significantly higher proportion than in healthy Japanese controls (38%, n = 1508; p = 0.018), but not in Japanese patients with RA (n = 759)[9].

Clinical course of patients with MTX-LPD. MTX was withdrawn in all cases at the time of LPD diagnosis. When examining the need for chemotherapy within 18 months of

Table 2. HLA-A, B, and DR alleles of 16 cases of RA with MTX-LPD.

No.	HLA-A	HLA-B	HLA-DR
1	11:01/24:02	35:01/48:01	04:05*/09:01
3	02:01/24:02	15:11/40:02	09:01/14:02*
4	24:02/26:01	15:07/40:02	04:03/09:01
5	24:02	07:02/52:01	01:01*/15:02
6	02:06/26:01	15:11/39:01	04:10*/14:06*
7	02:01/26:01	35:01/55:02	04:05*/04:06
9	24:02	07:02/54:01	04:05*/08:02
10	11:01	48:01/54:01	04:05*/15:01
11	02:01/02:07	15:11/46:01	09:01
12	24:02/26:01	40:02/52:01	04:05*/09:01
13	02:01/24:02	40:01/52:01	04:05*/15:02
14	24:02/33:03	44:03/52:01	08:03/15:02
15	24:02	52:01	15:02
18	02:01	07:02/15:01	01:01*/15:01
19	02:01/02:06	48:01/54:01	04:05*/04:07
20	24:02	51:01/59:01	01:01*/04:05*

* Rheumatoid arthritis shared epitope. RA: rheumatoid arthritis; MTX-LPD: methotrexate-associated lymphoproliferative disorders.

diagnosis, withdrawal of MTX alone was more successful for those in the EBVMCU group (n = 4, cases 1, 4, 5, and 21) than the other cases (n = 13; 75% vs 7.7%, p = 0.015; Figure 3). Because the observation periods were at most 2 years in the majority of cases, we were unable to calculate longterm prognosis. Five patients (cases 2, 7, 8, 9, and 12) died; LPD recurred in 2 patients at 90 months (case 9) and 21 months (case 12) from the original diagnosis and did not respond to continued chemotherapy. One patient (case 2) died from intercurrent myelitis and sepsis soon after the diagnosis of LPD and 1 patient (case 7) died from bleomycin-induced pneumonia.

One patient (case 8) was first diagnosed with EBV-positive small B cell lymphoma (SBL). Although chemotherapy resulted in partial remission, she had an indolent clinical course without chemotherapy until the tumor progressed and histopathological study revealed EBV-negative DLBCL with the same phenotype as the SBL. A clonal relationship between the 2 lymphomas was not proven; however, Richter syndrome was suspected clinically. With regard to the predicted unfavorable prognosis, she was treated with autologous peripheral blood stem cell transplantation, but she died of pneumocystis pneumonia under continuous immunosuppression. Although 2 cases of EBVMCU (cases 2 and 5) were included in Ann Arbor stage IV, each had a favorable clinical outcome.

DISCUSSION

We have shown that the presence of EBVMCU appears to confer a better prognosis in patients with MTX-LPD. Most of our patients with positive outcomes had been diagnosed with EBVMCU. Of the 12 cases of MTX-LPD with mucocutaneous ulcer reported in the literature[7,10,11,12,13,14,15,16,17] all except 1[17] were EBV-positive and all 9 cases with available data showed complete remission without chemotherapy.

EBVMCU was first reported to be a favorable prognostic indicator in a case series of 26 patients (consisting of 19 with Age-LPD and 7 with iatrogenic immunodeficiency-associated LPD including 4 with MTX-LPD)[7], but the incidence of EBVMCU in MTX-LPD was not known. Our study shows that the incidence of EBVMCU in EBV+ MTX-LPD is 42% (5 out of 12), which is higher than that of EBVMCU in Age-LPD (13%, 16 cases out of 122)[18].

Age-LPD is believed to be a consequence of an underlying immunological deficit, or immunosenescence of the T cell receptor (TCR) repertoire[19,20] — a natural degeneration of the immune system that occurs with aging. Considering the high average age of our cases, age-related immunosenescence might be partly involved in the development of MTX-LPD. This may be revealed by decreases in the TCR repertoire in the future.

Only a few cases of EBV latency in MTX-LPD have been reported; those of EBV latency among MTX-LPD, PT-LPD, and Age-LPD are summarized in Table 4[21,22,23]. Other case series include 53 cases of LPD in a variety of autoimmune diseases, including 4 cases of MTX-LPD, in which all 16 cases of EBV+ LPD were in latency II[24]. Taken together, these data suggest that EBV+ MTX-LPD is more

Table 3. Risk allele of RA with MTX-LPD in Japanese population.

	Total Allele Nos.	(+)	(–)	Frequency of Allele in Control Cases	p*	Pc Value**	OR	95% CI
HLA-B15:11								
in RA with MTX-LPD, n = 16	32	3	29	0.0096[1]	0.0036	0.061	10.0	3.0–32.8
				0.0052[2]	0.0097	0.16	18.5	1.9–183.4
in RA with MTX-LPD without EBVMCU, n = 13	26	3	23	0.0096[1]	0.0020	0.032	13.4	4.0–45.0
				0.0052[2]	0.0056	0.090	24.9	2.5–249.5
in EBV+ RA with MTX-LPD, n = 9	18	3	15	0.0096[1]	0.00066	0.0079	18.2	5.3–62.3
				0.0052[2]	0.0020	0.024	38.2	3.7–390.0

[1] Japanese healthy control. [2] RA control. * 2 × 2 Fisher's exact study. ** Corrected with Bonferroni's method. RA: rheumatoid arthritis; MTX-LPD: methotrexate-associated lymphoproliferative disorders; EBV: Epstein-Barr virus; EBVMCU: EBV-positive mucocutaneous ulcer.